JIPB Journal of Integrative Plant Biology

Decreased glutathione reductase2 leads to early leaf senescence in *Arabidopsis*

Shunhua Ding[1], Liang Wang[1,2], Zhipan Yang, Qingtao Lu[1], Xiaogang Wen[1] and Congming Lu[1]*

[1]Photosynthesis Research Center, Key Laboratory of Photobiology, Institute of Botany, Chinese Academy of Sciences, Beijing 100093, China, [2]University of Chinese Academy of Sciences, Beijing 100049, China. *Correspondence: lucm@ibcas.ac.cn

Abstract Glutathione reductase (GR) catalyzes the reduction of glutathione disulfide (GSSG) to reduced glutathione (GSH) and participates in the ascorbate-glutathione cycle, which scavenges H_2O_2. Here, we report that chloroplastic/mitochondrial GR2 is an important regulator of leaf senescence. Seed development of the homozygous *gr2* knockout mutant was blocked at the globular stage. Therefore, to investigate the function of GR2 in leaf senescence, we generated transgenic *Arabidopsis* plants with decreased GR2 using RNAi. The *GR2* RNAi plants displayed early onset of age-dependent and dark- and H_2O_2-induced leaf senescence, which was accompanied by the induction of the senescence-related marker genes *SAG12* and *SAG13*. Furthermore, transcriptome analysis revealed that genes related to leaf senescence, oxidative stress, and phytohormone pathways were upregulated directly before senescence in RNAi plants. In addition, H_2O_2 accumulated to higher levels in RNAi plants than in wild-type plants and the levels of H_2O_2 peaked in RNAi plants directly before the early onset of leaf senescence. RNAi plants showed a greater decrease in GSH/GSSG levels than wild-type plants during leaf development. Our results suggest that GR2 plays an important role in leaf senescence by modulating H_2O_2 and glutathione signaling in *Arabidopsis*.

Keywords: *Arabidopsis thaliana*; ascorbate-glutathione cycle; glutathione reductase2; hydrogen peroxide; leaf senescence
Citation: Ding S, Wang L, Yang Z, Lu Q, Wen X, Lu C (2016) Decreased glutathione reductase2 leads to early leaf senescence in *Arabidopsis*. **J Integr Plant Biol** 58: 29–47 doi: 10.1111/jipb.12371
Edited by: Chun-Ming Liu, Institute of Botany, CAS, China
Received Mar. 24, 2015; **Accepted** May 26, 2015
Available online on Jun. 1, 2015 at www.wileyonlinelibrary.com/journal/jipb
© 2015 The Authors. *Journal of Integrative Plant Biology* published by Institute of Botany, Chinese Academy of Sciences
This is an open access article under the terms of the Creative Commons Attribution-NonCommercial License, which permits use, distribution and reproduction in any medium, provided the original work is properly cited and is not used for commercial purposes.

Research Article

OnlineOpen

INTRODUCTION

Glutathione (γ-l-glutamyl-l-cysteinylglycine) is a multifunctional metabolite in plants. It is an important regulator of gene expression, cell signaling, the cell cycle, plant development, and cell death, and plays essential roles in processes such as glyoxylase and formaldehyde metabolism, sulfur assimilation, and the Calvin-Benson and Krebs cycles (Noctor et al. 2012). Glutathione exists in two forms: a reduced form (GSH) and an oxidized form (GSSG). Under normal growth conditions, more than 90% of the glutathione in plant cells is in the reduced form (Noctor et al. 2002). As most physiological functions of glutathione in plants are attributed to its reduced form (Alscher 1989), normal growth and development depend on the presence of a high proportion of GSH. GSH synthesis in chloroplasts and cytosols and reduction of GSSG to GSH by glutathione reductase (GR, EC 1.6.4.2) maintain high proportions of GSH (Noctor and Foyer 1998; Asada 1999).

GSSG is reduced to GSH by GR in the ascorbate-glutathione cycle, an important reactive oxygen species (ROS)-scavenging pathway present in almost all cellular compartments in plants (Mittler 2002). In this cycle, ascorbate peroxidase reduces H_2O_2 to water and concurrently oxidizes ascorbate to monodehydroascorbate. The reduction of monodehydroascorbate occurs via the catalytic action of monodehydroascorbate reductase, which uses NAD(P)H as an electron donor. Monodehydroascorbate can also disproportionate to dehydroascorbate and ascorbate. Dehydroascorbate can then be reduced to ascorbate by dehydroascorbate reductase, an enzyme that uses GSH as an electron donor, resulting in the formation of GSSG. GSSG in turn is re-reduced to GSH by GR, in a reaction that uses reduced form of nicotinamide adenine dinucleotide phosphate (NADPH) as an electron donor (Asada 1999; Foyer and Noctor 2005). Thus, GR maintains the cellular glutathione redox status and thereby protects plants against oxidative stress (Mittler 2002; Noctor et al. 2012).

Subcellular fractionation studies detected GR activities in the chloroplast, cytosol, mitochondria, and peroxisome in many plant species (Edwards et al. 1990; Jiménez et al. 1998; Kataya and Reumann 2010). GR activities differ both in different cellular compartments and in different species. In *Pisum sativum* (pea) and *Nicotiana tabacum* (tobacco) plants, most GR activity is found in the chloroplast. For example, in pea plants, about 77% of the total GR activity is in the chloroplast and only about 20% and 3% is in the cytosol and mitochondria, respectively (Edwards et al. 1990). In tobacco plants, about 70% of total GR activity is in the chloroplast (Ding et al. 2009). Two genes, *GR1* (At3g24170) and *GR2* (At3g54660), encode GR in *Arabidopsis*. The subcellular distribution of GR activities in *Arabidopsis* differs from that in pea and tobacco plants, with GR1 activity localizing to the cytosol and peroxisomes (Marty et al. 2009; Kataya and Reumann 2010) and GR2 to chloroplasts and mitochondria (Creissen et al. 1995; Chew et al. 2003; Yu et al. 2013). GR1 accounts for 40% to 65% of the total GR activity in *Arabidopsis* leaves (Marty et al. 2009; Mhamdi et al. 2010; Yu et al. 2013).

The possible roles of GR in different cellular compartments have been investigated extensively. Elevated levels of cytosolic GR activity in transgenic tobacco plants have no effect on the size of the glutathione pool and the reduction status of glutathione under optimal or oxidative conditions (Foyer et al. 1991). In *Arabidopsis*, GR1 does not affect plant development under normal growth conditions (Marty et al. 2009). However, GR1 plays an essential role in H_2O_2 metabolism and signaling (Mhamdi et al. 2010). By contrast, chloroplastic GR improves resistance to abiotic stresses. Transgenic tobacco, poplar, and *Gossypium hirsutum* (cotton) plants with enhanced chloroplastic GR activities had increased resistance to oxidative stress caused by ozone, paraquat, high light, or chilling stresses (Aono et al. 1993; Broadbent et al. 1995; Foyer et al. 1995; Payton et al. 2001; Kornyeyev et al. 2003). By contrast, tobacco plants with decreased chloroplastic GR activity were more sensitive than the wild type to oxidative stress caused by paraquat or chilling stresses (Aono et al. 1995; Ding et al. 2009, 2012). Moreover, mutation of *Arabidopsis GR2* is lethal in early embryo development (Tzafrir et al. 2004; Marty et al. 2009), suggesting that GR2 is crucial for several aspects of plant development, even under normal growth conditions. Indeed, recent work showed that GR2 is essential for root apical meristem maintenance in *Arabidopsis*, as it regulates the glutathione redox status under normal growth conditions (Yu et al. 2013).

To date, the functions of GR2 in leaf development remain unclear. Here, we report that *Arabidopsis GR2* regulates leaf senescence and embryo development. *GR2* RNAi plants showed early onset of age-dependent and dark- and H_2O_2-induced leaf senescence, accumulated high levels of H_2O_2, and exhibited enhanced sensitivity to H_2O_2. Transcriptome analysis revealed that the expression of genes related to oxidative stress, leaf senescence, and phytohormone pathways was upregulated in *GR2* RNAi plants. These results demonstrate that GR2 plays an important role in leaf senescence by modulating H_2O_2 and glutathione signaling in *Arabidopsis*.

RESULTS

GR2 is essential for embryo development

Previous work suggested that *GR2* deletion is embryonic lethal (Tzafrir et al. 2004). To investigate how *GR2* deletion affects embryo development, we examined the *gr2* mutant (Salk_040170), which contains a T-DNA insertion in exon 9 of At3g54660 (Figure S1A). We found no homozygous *gr2* mutant plants and heterozygous *gr2* plants showed a wild-type phenotype. Whereas the developing siliques of wild-type plants contained green seeds, those of heterozygous *gr2* plants contained both green and white seeds (Figure S1B). In mature siliques, the seeds of the *gr2* mutant were small and shriveled and could not germinate (Figure S1C). About one-quarter of the embryos were aborted, which is consistent with the trait being controlled by a single, recessive allele. To identify which stages of embryogenesis were arrested in the *gr2* mutant, we examined the embryos in the cleared seeds of a developmental series of siliques. We found that development of the homozygous *gr2* seeds was blocked at the globular stage, whereas embryos in wild-type and heterozygous *gr2* seeds underwent normal development (Figure S1D).

To confirm that *GR2* was responsible for the embryo-lethal phenotype of the *gr2* mutant, we introduced full-length *GR2* under the control of the 35S promoter into heterozygous *gr2* plants. The complemented plants showed normal embryonic development, as observed in wild-type plants (Figure S1B, C). Thus, this indicates that the mutation in *GR2* is responsible for the embryo-lethal phenotype of *gr2*.

GR2 is highly expressed in mature and senescent leaves

GR2 is expressed throughout the seedling and is widely expressed in various organs and tissues in *Arabidopsis*, including roots, leaves, flowers, and siliques (Yu et al. 2013). We examined the expression of *GR2* in developing young leaves, mature leaves, and senescent leaves, using the senescence-associated gene (*SAG*) *SAG13* as a senescence marker (Schippers et al. 2008). Reverse transcription-polymerase chain reaction (RT-PCR), GUS staining, and quantitative real-time PCR analyses showed that *GR2* was expressed throughout leaf development, but was highly expressed in mature and senescent leaves (Figure 1), suggesting that GR2 might be involved in leaf development.

Generation of transgenic plants with decreased *GR2* expression

To investigate the functions of GR2 in leaf development, we generated transgenic *Arabidopsis* plants with decreased levels of *GR2* using RNAi technology. We selected three independent RNAi lines (*igr2-7*, *igr2-9*, and *igr2-14*) with greatly reduced *GR2* mRNA levels and used the T4 progeny of these lines in subsequent analyses. Using 3-week-old seedlings, we compared the *GR2* mRNA levels, GR2 protein levels, and GR activity between wild-type and RNAi plants (Figure 2). *GR2* mRNA levels were significantly reduced in the three RNAi lines (Figure 2A, B). Quantitative real-time PCR showed that the level of *GR2* transcript was about 50% in *igr2-7* plants and about 10% in *igr2-9* and *igr2-14* compared to that in wild-type plants (Figure 2A, B). Immunoblot analysis using antiserum specific for *Arabidopsis* GR2 identified a protein band of about 58 kDa. The GR2 protein level in *igr2-7*, *igr2-9*, and *igr2-14* plants decreased to about 50, 10, and 10% of that in wild-type plants, respectively (Figure 2C). The total GR activity in the leaves of *igr2-7*, *igr2-9*, and *igr2-14* plants decreased to 70, 39, and 40% of that in wild-type plants, respectively (Figure 2D). GR1 was reported to account for 40%–65% of the total GR activity in *Arabidopsis* leaves (Marty et al. 2009; Mhamdi et al. 2010). Thus, GR2 activity is greatly inhibited in *igr2-9* and *igr2-14* plants.

Decreased GR2 promotes early leaf senescence

Whereas the *igr2-7* plants showed no aberrant phenotype, the *igr2-9* and *igr2-14* plants were smaller than the wild type (Figure 3A). The leaf area of *igr2-9* and *igr2-14* plants was about 40% less than that of wild-type plants at 30 d after seed germination (Figure 3B). Early leaf senescence symptoms were observed at the flowering stage in *igr2-9* and *igr2-14* plants, but not in the wild-type and *igr2-7* plants (Figure 3C). These results prompted us to investigate how GR2 influences leaf senescence. We harvested the fourth rosette leaves of wild-type and RNAi plants at the indicated time points. We

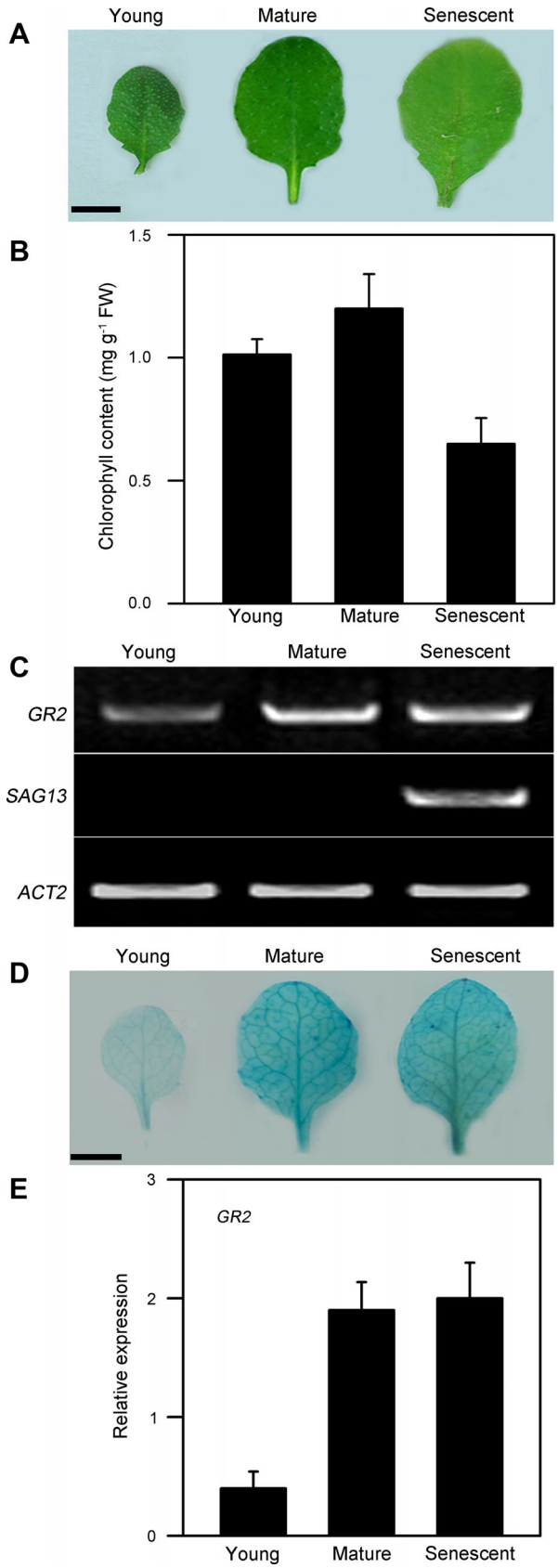

Figure 1. Continued.

observed early onset of leaf senescence in *igr2-9* and *igr2-14* plants (Figure 4A). Leaf senescence was further characterized by examining well-established physiological parameters for leaf senescence, including chlorophyll content, maximal efficiency of PSII photochemistry (F_v/F_m), malondialdehyde (MDA) content, and membrane ion leakage (Lim et al. 2007). Chlorophyll contents started to decrease at 45 d in wild-type plants but at 35 d in *igr2-9* and *igr2-14* plants. Moreover, *igr2-9* and *igr2-14* plants showed a greater decrease in chlorophyll levels than did the wild-type plants (Figure 4B). Similar results were observed for F_v/F_m in wild-type and *igr2-9* and *igr2-14* plants (Figure 4C). The MDA content started to increase at 40 d in wild-type plants, but already at 30 d in the *igr2-9* and *igr2-14* plants, and the increase was much greater in *igr2-9* and *igr2-14* plants than in wild-type plants (Figure 4D). The patterns for membrane ion leakage in wild-type and *igr2-9* and *igr2-14* plants were similar to those observed for MDA content (Figure 4E).

To further characterize early leaf senescence in *igr2-9* and *igr2-14* plants, we examined the expression of two established senescence marker genes, *SAG12* and *SAG13* (Figure 4F, G). *SAG13* expression, which is associated with oxidative stress and senescence (Weaver et al. 1998), was detected starting at day 35 in *igr2-9* and *igr2-14* plants, but only starting at day 45 in wild-type plants. *SAG13* expression in *igr2-9* and *igr2-14* plants was about 200-fold higher at day 50 than in wild-type plants (Figure 4F). Expression of *SAG12*, a hallmark of age-induced senescence (Weaver et al. 1998), was detected starting at day 40 in *igr2-9* and *igr2-14* plants, but starting at day 50 in wild-type plants. At day 55, *SAG12* expression was about 80-fold higher in *igr2-9* and *igr2-14* plants than in the wild type (Figure 4G).

Decreased GR2 leads to a change in glutathione redox status during leaf development

Glutathione reductase regulates the redox status of glutathione pools, indicated as the GSH/GSSG ratio, by catalyzing the reduction of GSSG. To investigate how decreased GR2 affects the GSH/GSSG ratio during leaf development, we measured the glutathione pools in wild-type and RNAi plants (Figure 5). We found that total glutathione (GSH + GSSG), GSH, and GSSG contents increased gradually in young leaves during leaf development, peaked in mature leaves, and then decreased considerably in senescent leaves in wild-type and

◀ **Figure 1. *GR2* expression in young, mature, and senescent leaves in wild-type plants**

(A) Morphologies of young, mature, and senescent leaves. Bars = 5 mm. **(B)** Chlorophyll contents in young, mature, and senescent leaves. **(C)** Reverse transcription-polymerase chain reaction (RT-PCR) analysis of *GR2* and *SAG13* expressions in young, mature, and senescent leaves. *ACT2* was used as the loading control. **(D)** $GR2_{pro}$*:GUS* expression in young, mature, and senescent leaves. Bars = 5 mm. **(E)** Transcript levels of *GR2* were determined by real-time PCR using *ACT2* as an internal control. The fourth rosette leaves of wild-type plants grown in soil were used. The young, mature, and senescent leaves were analyzed at 10, 35, and 55 d after emergence, respectively. The values are means ± *SD* of three independent experiments.

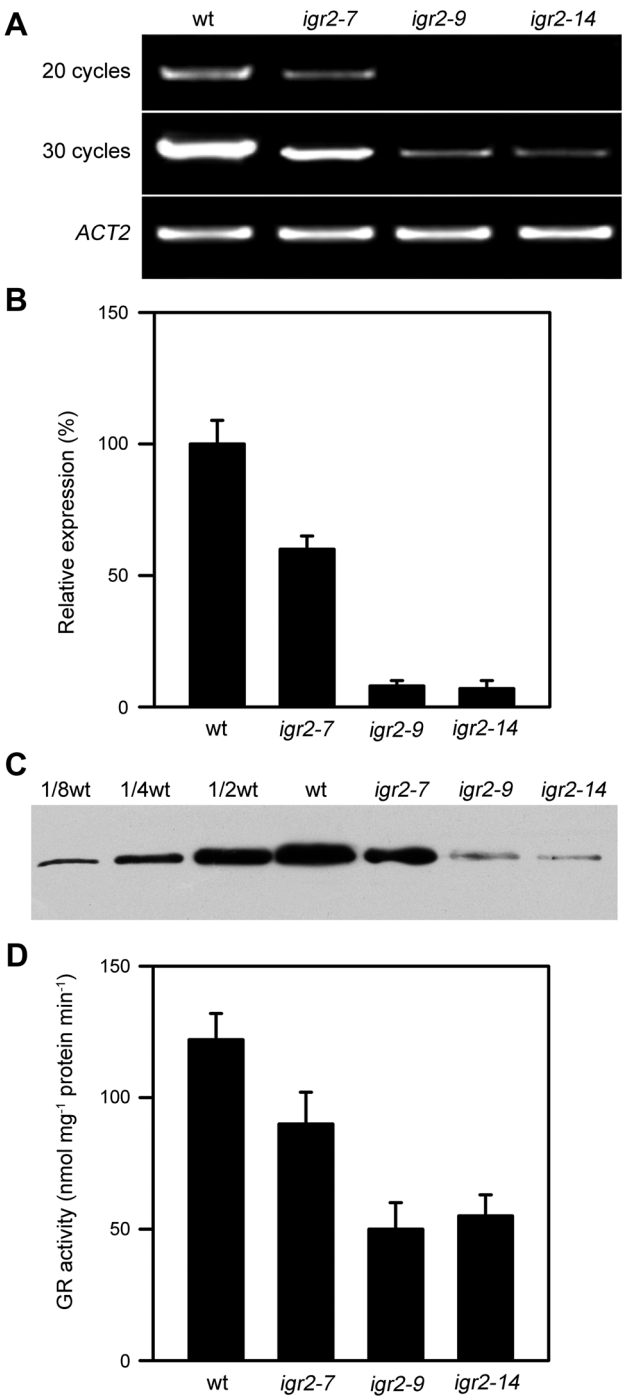

Figure 2. The levels of *GR2* mRNA, GR2 protein, and total glutathione reductase (GR) activity in wild-type (wt) and *GR2* RNAi (*igr2-7*, *igr2-9*, and *igr2-14*) plants

(A) *GR2* mRNA levels determined by RT-PCR. **(B)** *GR2* mRNA levels analyzed by real-time PCR. **(C)** GR2 protein levels. **(D)** Total GR activity. Three-week-old seedlings were used to compare *GR2* mRNA levels, GR2 protein levels, and total GR activity between wt and RNAi plants. Specific primers used are listed in Table S1. The values shown are means ± *SD* of three independent experiments.

RNAi plants (Figure 5A–C). However, total glutathione, GSH, and GSSG contents peaked much earlier in *igr2-9* and *igr2-14* plants than in wild-type plants. Total glutathione and GSH contents peaked at 20 d after leaf emergence in *igr2-9* and *igr2-14* plants, but at 35 d in wild-type plants. GSSG content peaked at 35 d in *igr2-9* and *igr2-14* plants, but at 45 d in wild-type plants. In addition, the increase in total glutathione, GSH, and GSSG contents in young leaves was much greater in *igr2-9* and *igr2-14* plants than in wild-type plants. By contrast, the decrease in GSH and GSSG contents in senescent leaves was much greater in *igr2-9* and *igr2-14* plants than in wild-type plants. The GSH/GSSG ratio decreased with leaf development in wild-type and RNAi plants and the decrease was much greater in *igr2-9* and *igr2-14* plants than in wild-type plants. Moreover, the GSH/GSSG ratio was much lower in *igr2-9* and *igr2-14* plants than in wild-type plants (Figure 5D). Similar changes in glutathione content during leaf senescence have been reported in *Arabidopsis* and *Triticum aestivum* (wheat) (Pavet et al. 2005; Li et al. 2014).

Decreased GR2 results in elevated levels of H_2O_2

The reaction catalyzed by GR is part of the ascorbate-glutathione cycle, which scavenges H_2O_2 (Asada 1999). Therefore, we monitored the levels of reactive oxygen species (ROS), including H_2O_2, superoxide ($O_2^{\bullet-}$), and singlet oxygen ($^1O_2$), during leaf development in wild-type and RNAi plants (Figure S2). DAB (3,3′-diaminobenzidine tetrachloride) staining showed that the level of H_2O_2 increased slightly with leaf development and peaked at around 40 d after leaf emergence in wild-type plants, whereas the level of H_2O_2 peaked at 30 d and then decreased slightly in *igr2-9* and *igr2-14* plants. Furthermore, the level of H_2O_2 was greater in *igr2-9* and *igr2-14* plants than in wild-type plants (Figure S2A). NBT (4-nitroblue tetrazolium chloride) staining and Singlet Oxygen Sensor Green (SOSG) fluorescence analysis showed that the levels of $O_2^{\bullet-}$ and $^1O_2$ remained low in young leaves and increased after leaf maturation in wild-type and *GR2* RNAi plants. There was no difference in the levels of $O_2^{\bullet-}$ and $^1O_2$ in young or senescent leaves between wild-type and *igr2-9* and *igr2-14* plants (Figure S2B, C).

We then quantified the level of H_2O_2 using an improved spectrophotometric assay (Figure 6). The H_2O_2 contents both in young and senescent leaves were higher in *igr2-9* and *igr2-14* plants than in wild-type plants. The H_2O_2 content increased rapidly in the young leaves of *igr2-9* and *igr2-14* plants and peaked at 30 d after leaf emergence. However, in the young leaves of wild-type plants, the H_2O_2 content increased slowly, peaked at 40 d, and then decreased slightly. Taken together, these results show that H_2O_2 accumulates to higher levels in the leaves of *igr2-9* and *igr2-14* plants than in wild-type plants during development.

Decreased GR2 leads to accelerated darkness- and H_2O_2-induced leaf senescence

H_2O_2 accumulation has been proposed to function as a signal in senescence in *Arabidopsis* (Foyer and Noctor 2005; Zentgraf and Hemleben 2008; Smykowski et al. 2010). Thus, the early leaf senescence observed in *igr2-9* and *igr2-14* plants may be associated with elevated levels of H_2O_2. To further examine

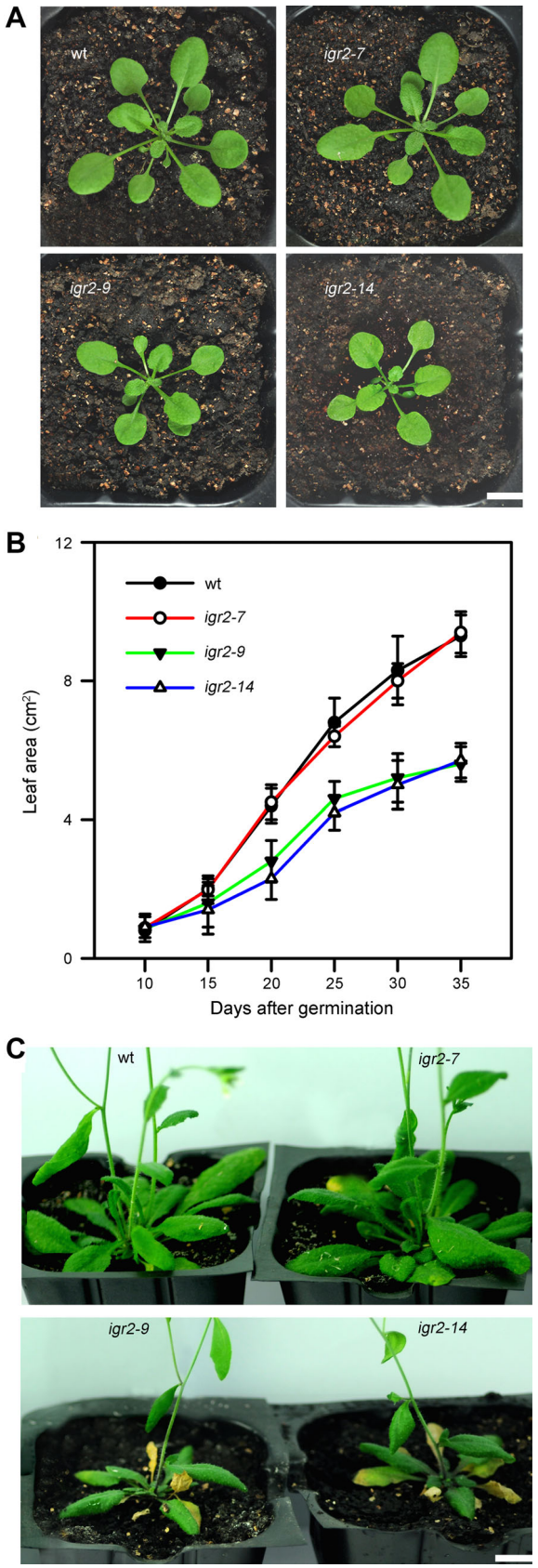

Figure 3. Continued.

this possibility, we investigated the response of wild-type and RNAi plants to a 3-d exposure to elevated H_2O_2 (10 mM) (Figure 7). To quantify the leaf senescence induced by elevated H_2O_2, we examined the four physiological parameters and two senescence marker genes described above in the fourth rosette leaves at 20 d after emergence. Indeed, we detected signs of senescence in the leaves of *igr2-9* and *igr2-14* plants (Figure 7A). Elevated H_2O_2 induced a decrease in chlorophyll and F_v/F_m and an increase in MDA content and membrane ion leakage in wild-type and RNAi plants. However, compared to wild-type plants, *igr2-9* and *igr2-14* plants showed a greater decrease in chlorophyll content and F_v/F_m and a greater increase in MDA content and membrane ion leakage (Figure 7B). In addition, the expression of *SAG13* and *SAG12* was higher in *igr2-9* and *igr2-14* plants than in wild-type plants after exposure to elevated levels of H_2O_2 (Figure 7C). These results indicate that the leaves of *igr2-9* and *igr2-14* plants are more sensitive to H_2O_2-inducible senescence than are those of wild-type plants.

Continuous darkness can induce leaf senescence in whole plants and detached leaves (Lin and Wu 2004; Chen et al. 2011). Therefore, we next examined whether GR2 is also involved in darkness-induced leaf senescence (Figure 8). After dark treatment, the leaves of *igr2-9* and *igr2-14* plants were more yellow than those of wild-type plants (Figure 8A). Darkness resulted in a decrease in chlorophyll contents and F_v/F_m, an increase in MDA contents, and membrane leakage in wild-type and RNAi plants. However, there was a greater decrease in chlorophyll content and F_v/F_m and a greater increase in MDA content and membrane leakage in *igr2-9* and *igr2-14* plants than in wild-type plants (Figure 8B). We also measured *SAG12* and *SAG13* mRNA levels by real-time PCR and found that these genes were induced earlier and to a greater extent in leaves of *igr2-9* and *igr2-14* plants than those in wild-type plants (Figure 8C). In addition, H_2O_2 accumulated to greater levels in *igr2-9* and *igr2-14* plants than in wild-type plants during dark treatments (Figure 8D). These results suggest that decreased GR2 also promotes darkness-induced leaf senescence.

We further investigated whether *GR2* expression is induced by elevated H_2O_2 exposure and continuous darkness. Detached leaves of wild-type plants (3-week-old seedlings) were treated with 10 mM H_2O_2 and continuous darkness. *GR2* expression was induced 6 h after exposure to H_2O_2 and levels of expression remained high for 3 d in the presence of H_2O_2 (Figure S3A). In addition, *GR2* expression was induced 12 h after exposure to continuous darkness and levels remained elevated until 5 d after exposure to continuous darkness (Figure S3B). These data suggest that *GR2* regulates the leaf senescence induced both by elevated H_2O_2 and continuous darkness.

◀ **Figure 3. The phenotypes and growth kinetics of wild type (wt) and *GR2* RNAi (*igr2-7*, *igr2-9*, and *igr2-14*) plants**
(A) Three-week-old plants. Bars = 1 cm. **(B)** Growth kinetics of wt and RNAi plants. The total leaf area was determined at the indicated days after seed germination. The values shown are means ± *SD* of three independent experiments. **(C)** Eight-week-old plants. Bars = 1 cm.

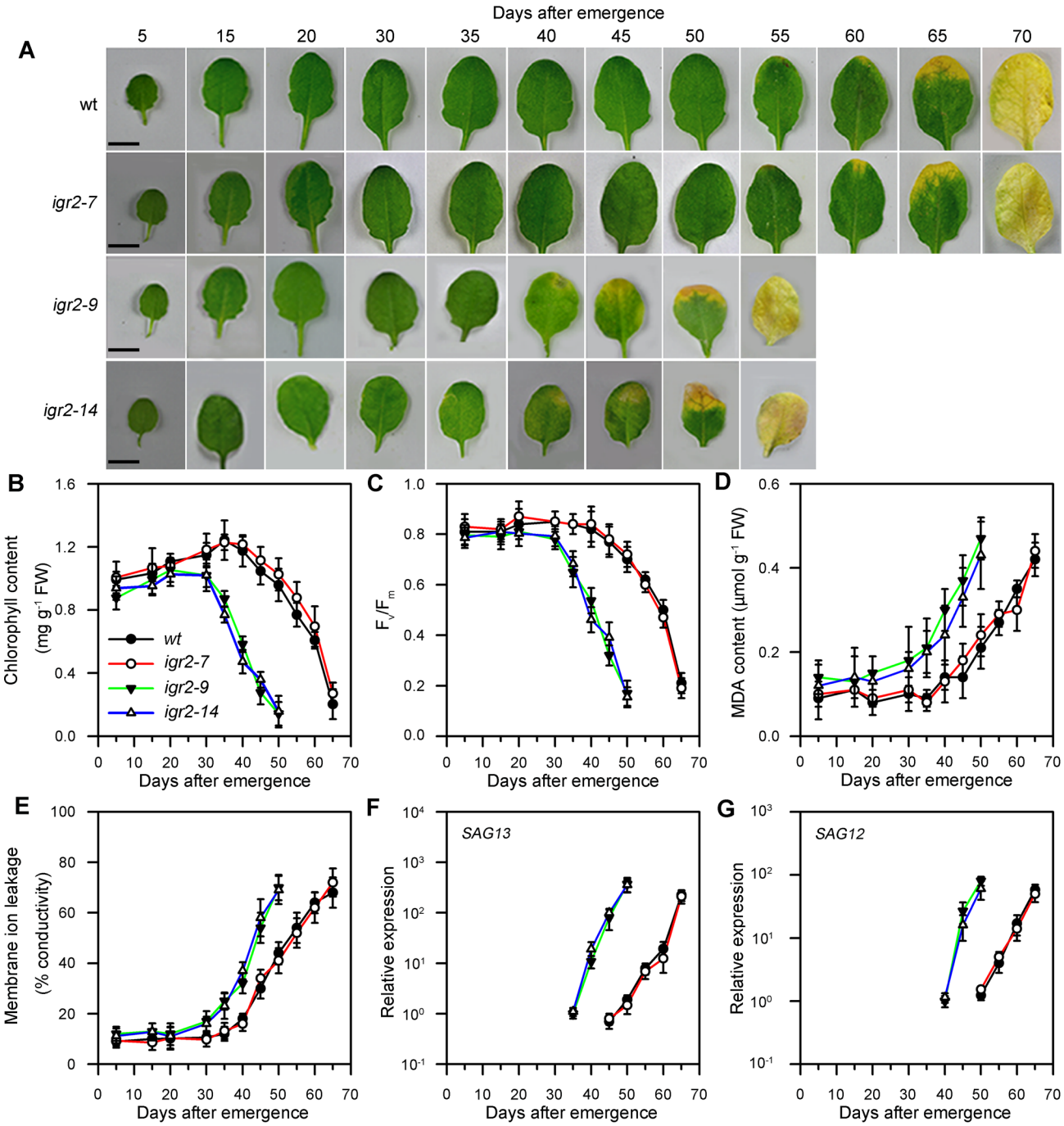

Figure 4. Age-dependent senescence in wild-type (wt) and *GR2* RNAi (*igr2-7*, *igr2-9*, and *igr2-14*) plants
(A) Morphologies of leaves. Bars = 5 mm. **(B, C, D, and E)** Measurements of chlorophyll content, F_v/F_m, malondialdehyde (MDA) content, and membrane ion leakage. **(F, G)** Expression of the senescence-related marker genes, *SAG12* and *SAG13*. Transcript levels were determined by real-time PCR using *ACT2* as an internal control. For *SAG13*, the relative transcript levels detected at day 35 in *igr2-9* plants were assigned a value of 1 after normalization to *ACT2* transcript levels. For *SAG12*, the relative transcript levels detected at day 40 in the *igr2-9* plant were assigned a value of 1 after normalization to *ACT2* transcript levels. The fourth rosette leaves from wt and RNAi plants grown in soil were sampled at the indicated days after emergence. The values are means ± *SD* of three independent experiments.

Decreased GR2 induces the expression of genes related to oxidative stress, senescence, and phytohormones

To examine the function of GR2, we conducted microarray experiments that compared the transcriptome profiles of the fourth leaves (at 20 d after emergence) of wild-type and *igr2-9* plants. At this age, there was no visible sign of leaf senescence. We selected genes that were differentially expressed (with a ≥2-fold change cut-off) in wild-type and

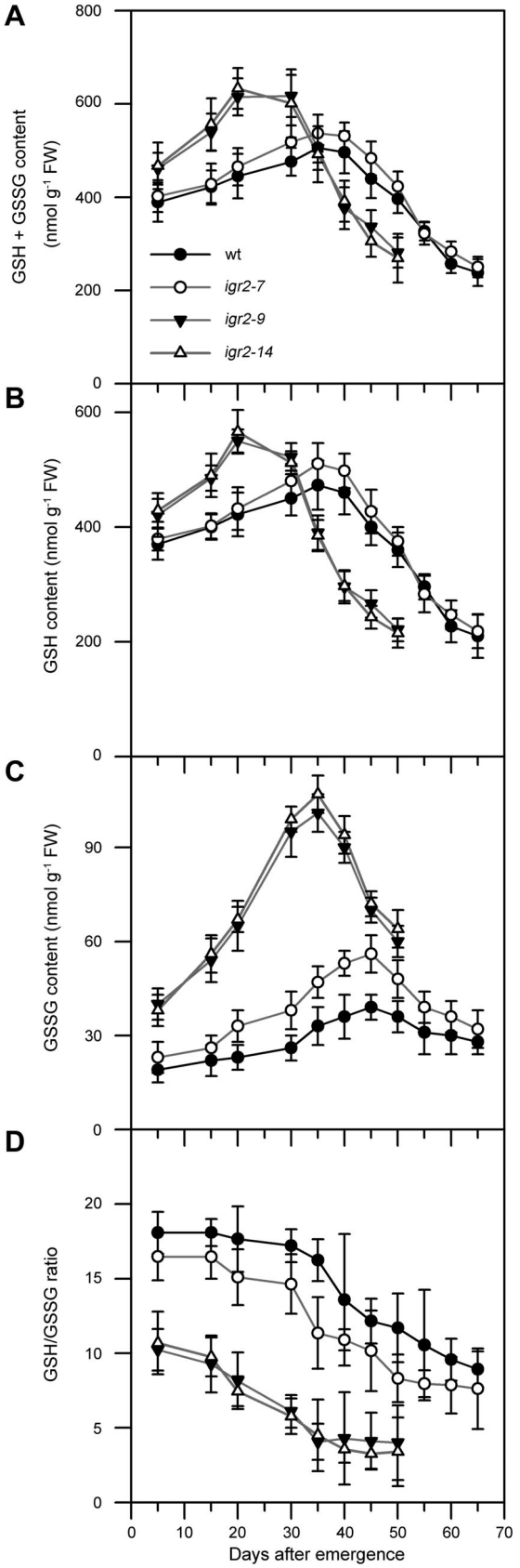

Figure 5. Continued.

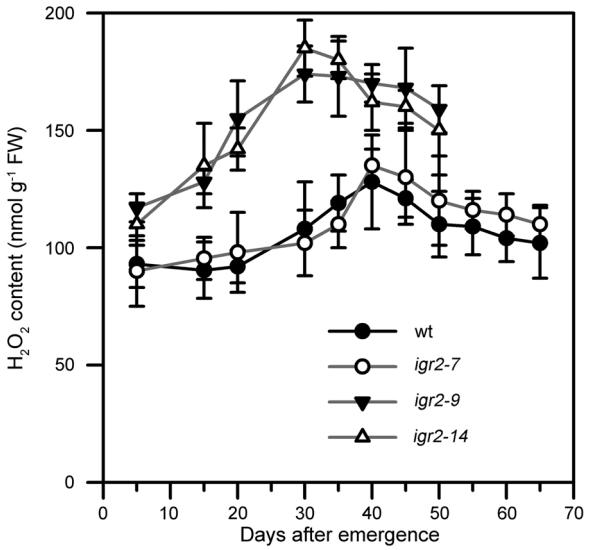

Figure 6. H_2O_2 levels in wild-type (wt) and *GR2* RNAi (*igr2-7*, *igr2-9*, and *igr2-14*) plants during leaf development
The fourth rosette leaves of wt and RNAi plants grown in soil were harvested at the indicated days after emergence and used for H_2O_2 measurements. The values are means ± *SD* of four to six independent experiments.

igr2-9 plants for GO analysis. We conducted a Fisher's test to calculate the significance of the percentage distribution of GO annotations for comparison with those in the whole genome (Figure 9). We identified 494 genes that were upregulated and 629 genes that were downregulated genes in *igr2-9* compared with wild-type plants (Table S2). Genes upregulated by decreased *GR2* expression had GO annotations highly associated with "response to stress" and "response to abiotic or biotic stimulus", with a *P*-value of 2.21×10^{-15} and 1.63×10^{-9}, respectively (Figure 9A), suggesting that stress-responsive genes are overrepresented in *igr2-9* plants. Furthermore, genes upregulated by decreased *GR2* expression were highly related to "response to oxidative stress", "defense response", and "leaf senescence", with *P*-values of 2.05×10^{-30}, 1.64×10^{-7}, and 2.24×10^{-4}, respectively (Figure 9B). In addition, genes upregulated by decreased *GR2* expression were highly related to "salicylic acid and jasmonic acid mediated signaling pathways" and to "responses to ethylene, jasmonic acid, salicylic acid, and abscisic acid stimulus" (Figure 9B). These results suggest that GR2 regulates the response to oxidative stress, leaf senescence, and

◀

Figure 5. Changes in glutathione pool size in wild-type (wt) and *GR2* RNAi (*igr2-7*, *igr2-9*, and *igr2-14*) plants during leaf development
(A) GSH + GSSG content. **(B)** GSH content. **(C)** GSSG content. **(D)** GSH/GSSG ratio. The fourth rosette leaves from wt and RNAi plants grown in soil were harvested at the indicated days after emergence and used for glutathione extraction. Six independent biological replicates were performed. The values are means ± *SD* ($n = 6$).

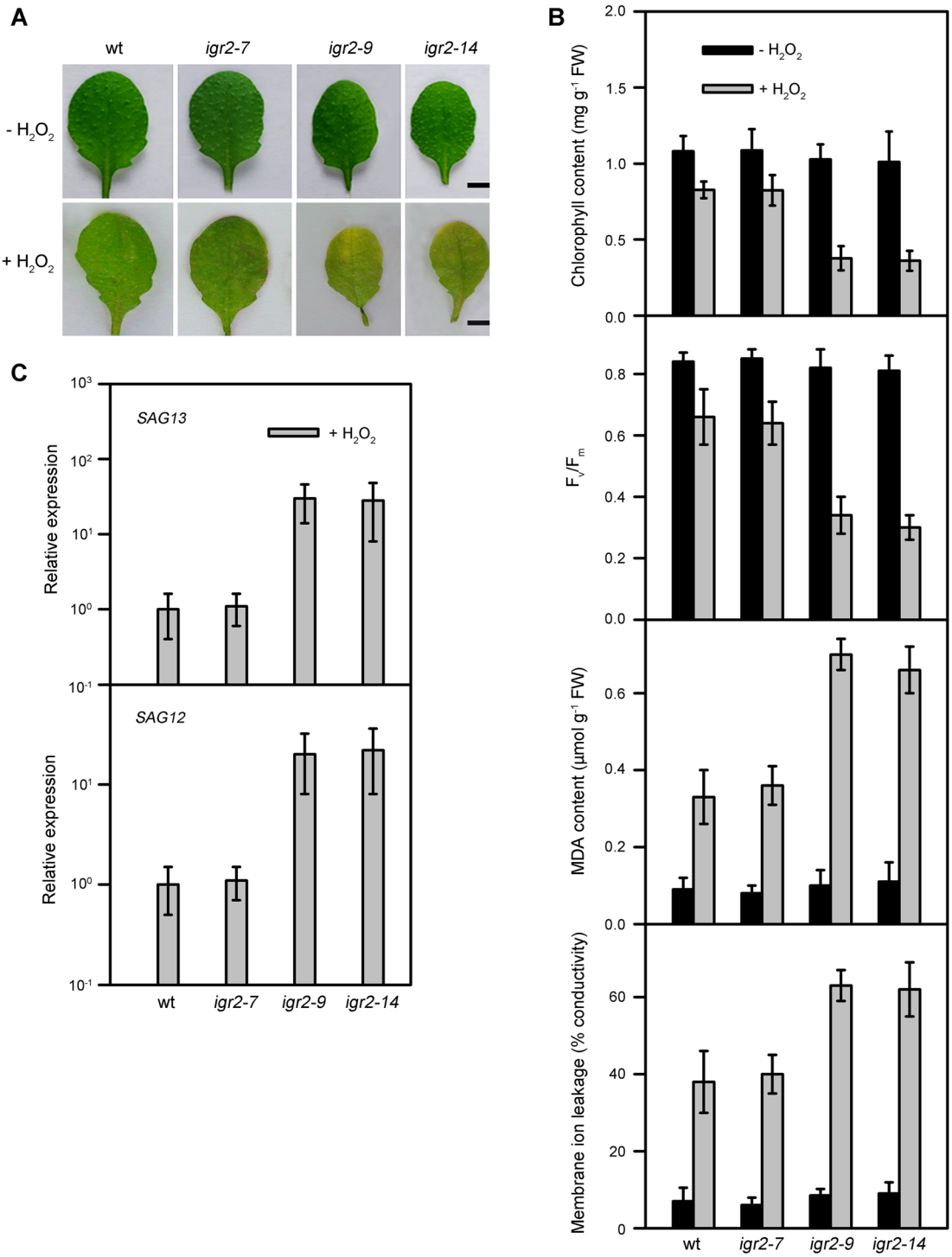

Figure 7. Effects of 10 mM H_2O_2 on detached leaves from wild-type (wt) and *GR2* RNAi (*igr2-7*, *igr2-9*, and *igr2-14*) plants
(A) Morphologies of leaves. Bars = 5 mm. **(B)** Chlorophyll content, F_v/F_m, MDA content, and membrane ion leakage. **(C)** Expression of the senescence-related marker genes, *SAG12* and *SAG13*. Transcript levels were determined by real-time PCR using *ACT2* as an internal control. For *SAG13*, the relative transcript levels detected in wt after H_2O_2 treatments were assigned a value of 1 after normalization to the *ACT2* transcript levels. For *SAG12*, the relative transcript levels detected in wt after H_2O_2 treatments were assigned a value of 1 after normalization to the *ACT2* transcript levels. *SAG12* and *SAG13* expression was not detected in wt and RNAi plants in the absence of the H_2O_2 treatment. The fourth rosette leaves at 20 d after emergence were used in the experiments. The values are means ± *SD* of three independent experiments.

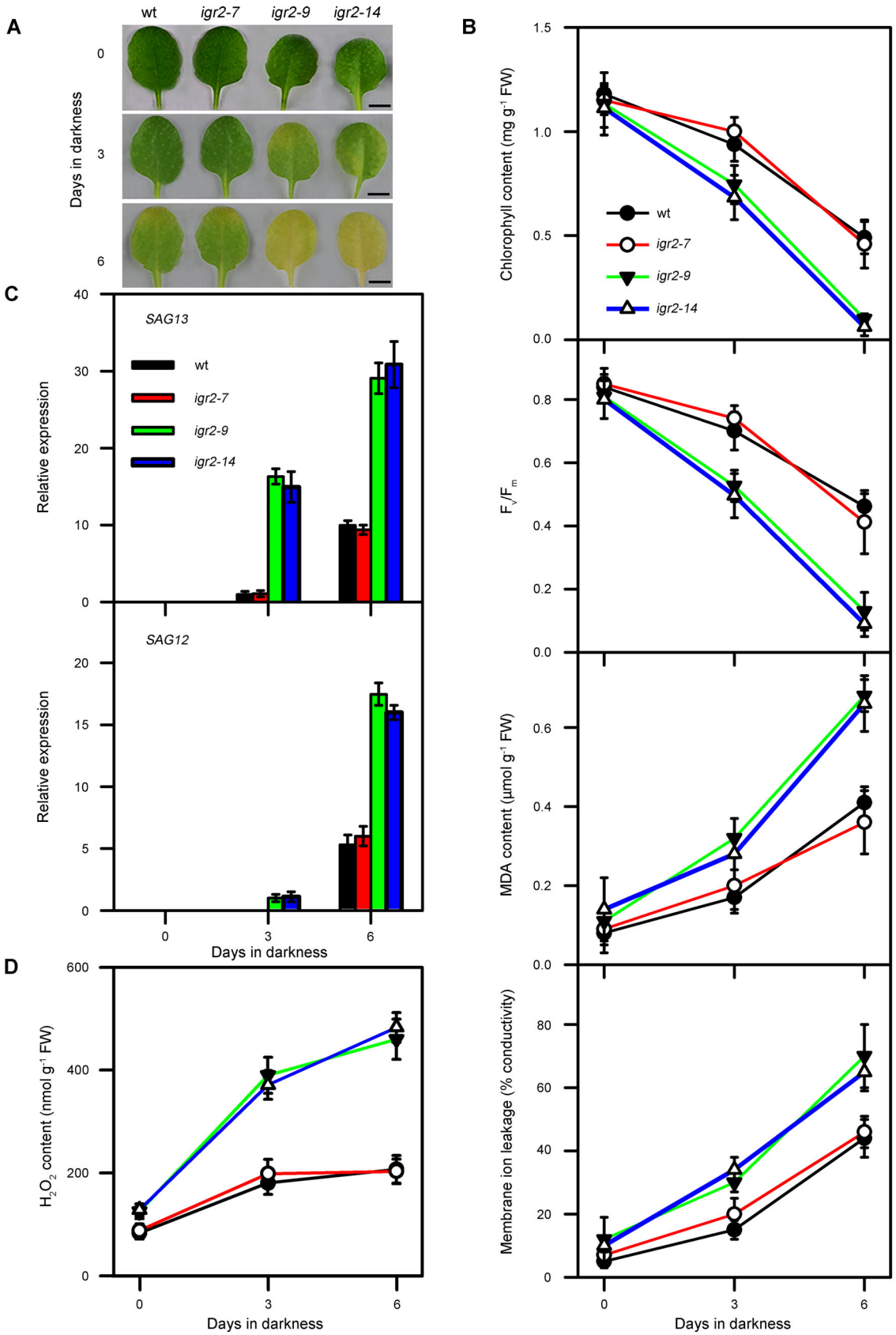

Figure 8. Continued.

phytohormone pathways. Further analysis indicated that several groups of genes involved in "response to high light", "response to heat", "response to wounding", and "response to water deprivation" were significantly overrepresented in *igr2-9* plants as compared to the whole genome. However, GR2 may not be involved in all types of stress response, such as cold stress since genes involved in cold stress were not affected in *igr2-9* plants (Figure 9B).

To confirm that genes identified as being differentially expressed in the microarray analysis were indeed up- or downregulated in *igr2-9* plants, we examined the expression of selected genes by real-time PCR (Table 1). Senescence-related genes, such as *NAC053*, *WRKY53*, *SEN1*, and *NAC2*, were about 6-, 10-, 7-, and 7-fold more strongly expressed, respectively, in *igr2-9* plants than in the wild type. The expression of oxidative stress-related genes, such as *GRXS13*, *CDSP32*, and *APX2*, and several defense-related genes, such as *SOT12*, *PR1*, and *HYS1*, were upregulated in *igr2-9* plants. In addition, the expression of phytohormone-related genes, such as *ERF1*, *PDF1.2A*, *ERF13*, *WRKY50*, and *EDL3*, were upregulated in *igr2-9* plants. Therefore, these results suggest that decreased GR2 may induce the expression of oxidative stress-, senescence-, and phytohormone-related genes before senescence.

DISCUSSION

Glutathione reductase reduces GSSG to GSH in the ascorbate-glutathione cycle, which scavenges H_2O_2 (Foyer and Noctor 2009). *Arabidopsis* GR1 is localized to the cytosol and peroxisomes. GR1 is not required for growth in optimal conditions but plays an important role when intracellular H_2O_2 production is increased and during pathogen challenge (Marty et al. 2009; Kataya and Reumann 2010; Mhamdi et al. 2010). *Arabidopsis* GR2 localizes to chloroplasts and mitochondria (Creissen et al. 1995; Chew et al. 2003). Many studies have shown that chloroplastic GR plays an important role in protecting plants against environmental and oxidative stresses (Aono et al. 1993, 1995; Foyer et al. 1995; Broadbent et al. 1995; Payton et al. 2001; Kornyeyev et al. 2003; Ding et al. 2009, 2012). Moreover, GR2 plays important roles in several aspects of plant development, since mutation of *GR2* is embryo lethal (Tzafrir et al. 2004; Marty et al. 2009) and GR2 is essential for root apical meristem maintenance (Yu et al. 2013). Our results confirmed that GR2 is essential for embryo development (Figure S1). The *gsh1* mutation, which disrupts glutathione synthesis, was also shown to be embryo lethal, but seed development of the homozygous *gsh1* mutant was blocked at the torpedo stage (Cairns et al. 2006). This suggests that a deficiency in GR2 leads to embryo lethality through a different mechanism from deficiency in GSH synthesis. We showed that a reduction in GR2 results in early onset of age-dependent and dark- and H_2O_2-induced leaf senescence (Figures 3, 4, 7 and 8). Thus, GR2 is an important regulator of leaf senescence in *Arabidopsis*. However, the expression pattern of *GR2* did not affect the onset of age-dependent leaf senescence in the wild type, since *GR2* is already highly expressed in mature leaves (Figure 1). The finding that growth of *GR2* RNAi seedlings was retarded (Figure 3B) suggests that *GR2* may promote growth.

How does GR2 regulate leaf senescence? Our results showed that large reductions in GR2 increased H_2O_2 accumulation in developing young leaves, mature leaves, and senescent leaves (Figure 6), indicating that GR2 is important for maintaining H_2O_2 homeostasis during leaf development in *Arabidopsis*. However, H_2O_2 accumulation varies throughout leaf development in *GR2* RNAi plants. The level of H_2O_2 increased significantly in the developing young leaves of *GR2* RNAi plants, peaking at 30 d after leaf emergence and then declining gradually (Figure 6). Leaf senescence commenced directly after H_2O_2 levels peaked in *GR2* RNAi plants, as reflected by a decrease in chlorophyll content and F_v/F_m, an increase in MDA content and membrane ion leakage, and an induction of the senescence marker genes, *SAG12* and *SAG13* (Figure 4, 6). In addition, we observed that the leaves of *GR2* RNAi plants turned yellow more rapidly than did those of wild-type plants following exposure to elevated levels of H_2O_2. The changes in the physiological parameters for leaf senescence further confirmed that *GR2* RNAi plants underwent early onset of leaf senescence in response to elevated H_2O_2 levels (Figure 7). Furthermore, the endogenous levels of H_2O_2 were higher in detached leaves from *GR2* RNAi plants than in those from the wild-type plants when senescence-inducing dark treatment was applied (Figure 8D). As expected, compared with wild-type leaves, the leaves of *GR2* RNAi plants showed an early senescence phenotype in response to darkness treatment, which was accompanied by a greater decrease in chlorophyll content and F_v/F_m and a greater increase in MDA content and membrane ion leakage as well as a greater increase in the expression of *SAG12* and *SAG13* (Figure 8A, B). Moreover, *GR2* was highly expressed in wild-type senescent leaves (Figure 1). Taken together, these results suggest that early onset leaf senescence in *GR2* RNAi plants is associated with H_2O_2 accumulation.

Was early onset of leaf senescence in *GR2* RNAi plants due to physiochemical damage to the cell caused by elevated H_2O_2 or, alternatively, could elevated H_2O_2 levels in *GR2* RNAi plants act as a signal that activates the gene expression pathways

◀

Figure 8. Effects of darkness on detached leaves from wild-type (wt) and *GR2* RNAi (*igr2-7*, *igr2-9*, and *igr2-14*) plants
(A) Morphologies of leaves. Bars = 5 mm. **(B)** Chlorophyll content, F_v/F_m, MDA content, and membrane ion leakage. The values are means ± *SD* of three independent experiments. **(C)** Expression of the senescence-related marker genes, *SAG12* and *SAG13*. Transcript levels were determined by real-time PCR using *ACT2* as an internal control. For *SAG13*, the relative transcript levels detected in wt after 3 d of dark treatment were assigned a value of 1 after normalization to *ACT2* transcript levels. For *SAG12*, the relative transcript levels detected in the *igr2-9* after 3 d dark treatments were assigned a value of 1 after normalization to the *ACT2* transcript levels. The values are means ± *SD* of three independent experiments. **(D)** H_2O_2 levels. The values are means ± *SD* of four to six independent experiments. The fourth rosette leaves at 20 d after emergence were used for dark treatments.

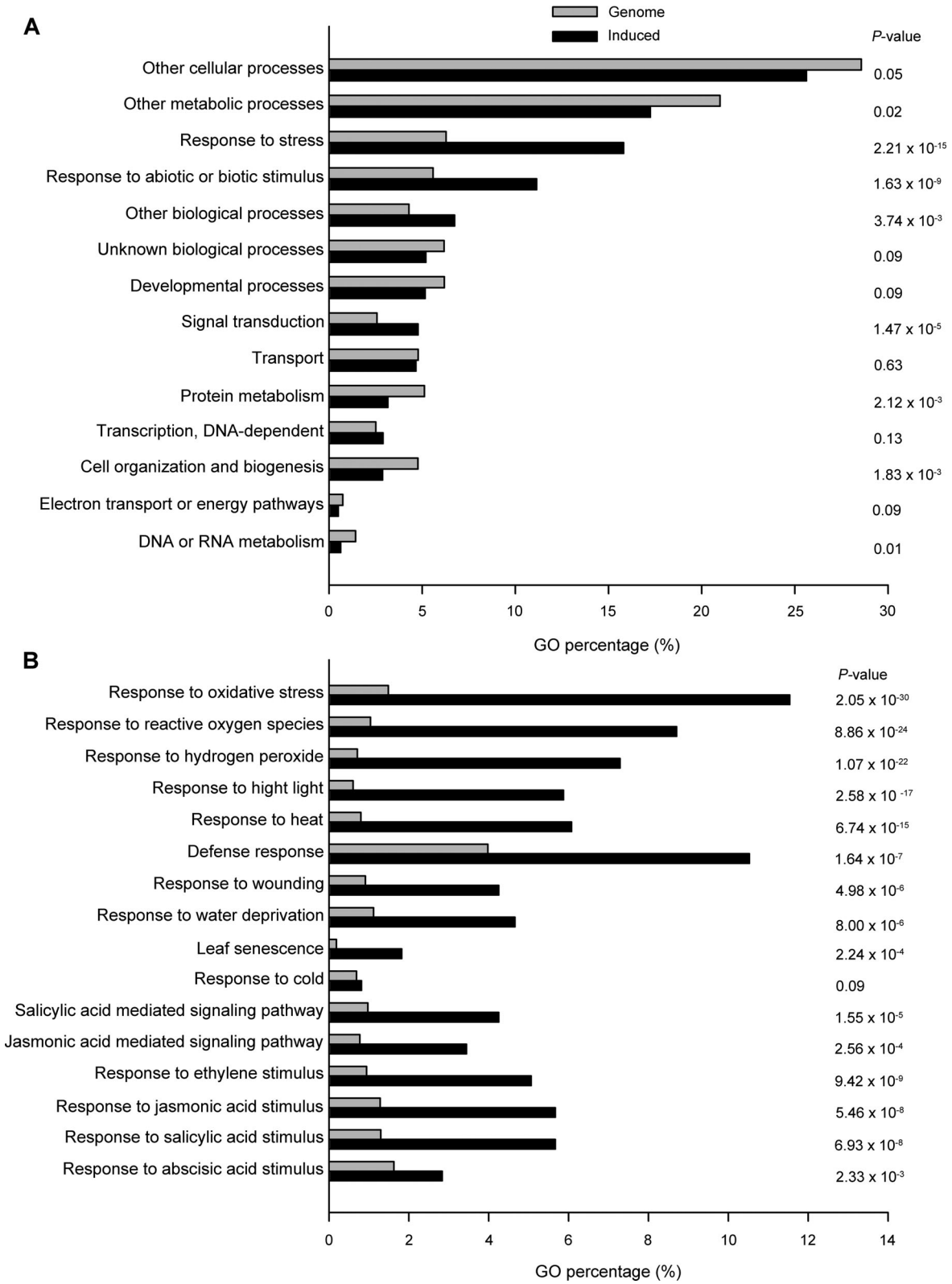

Figure 9. Global analysis of gene expression profiles in the *igr2-9* line
(A) Expression profiles of genes up-regulated in the *igr2-9* based on the gene ontology (GO) annotation (biological process) in TAIR. **(B)** Analysis of genes induced in *igr2-9* by specific GO terms. The fourth rosette leaves (at 20 d after emergence) were used for the microarray analysis. *P*-values in A and B were calculated by Fisher's test to compare the percentage distribution of GO annotation from genes induced by decreased *GR2* and the whole genome.

Table 1. Genes related to senescence, oxidative stress, defense, and phytohormones are upregulated in the fourth rosette leaves at 20 d after emergence in the *igr2-9* line

AGI number	Description	Fold change[a]	RER[b]
Senescence			
AT3G10500	NAC053	2.52	5.92 ± 0.4
AT4G23810	WRKY transcription factor 53 (WRKY53)	2.27	9.83 ± 1.7
AT4G35770	Senescence 1 (SEN1)	2.12	7.35 ± 1.2
AT5G39610	NAC2	2.17	7.29 ± 1.9
Oxidative stress			
AT1G02930	Glutathione transferase	2.00	6.03 ± 1.7
AT1G03850	Glutaredoxin (GRXS13)	2.72	5.46 ± 0.9
AT1G76080	Thioredoxin (CDSP32)	3.64	9.64 ± 1.7
AT3G09640	L-ascorbate peroxidase (APX2)	2.98	5.18 ± 1.9
AT4G16270	Peroxidase superfamily protein	2.84	8.15 ± 1.2
AT5G39580	Peroxidase superfamily protein	2.97	16.42 ± 1.8
Defense response			
AT2G03760	Brassinosteroid sulfotransferase (SOT12)	2.63	7.22 ± 1.4
AT2G14610	Pathogenesis-related gene1 (PR1)	2.97	7.34 ± 0.9
AT3G26830	Phytoalexin deficient (PAD3)	2.25	5.66 ± 1.4
AT4G12470	Azelaic acid induced 1 (AZI1)	2.62	7.65 ± 1.1
AT5G46050	Peptide transporter PTR3-A (PTR3)	2.27	8.05 ± 1.5
AT5G64930	Regulator of pathogenesis-related (HYS1)	2.66	6.00 ± 1.7
AT3G57240	Beta-1,3-glucanase 3 (BG3)	4.58	7.92 ± 1.2
Phytohormone pathway			
AT4G11890	Protein kinase family protein (ARCK1)	2.07	4.66 ± 0.4
AT2G13810	AGD2-like defense response protein 1 (ALD1)	2.66	5.50 ± 0.9
AT3G23240	Ethylene response factor1 (ERF1)	3.77	10.42 ± 0.9
AT5G44420	Plant defensin (PDF1.2A)	3.34	7.92 ± 1.2
AT2G44840	Ethylene-responsive element binding factor 13 (ERF13)	2.21	5.72 ± 1.3
AT2G19190	Senescence-induced receptor-like serine/threonine-protein kinase (FRK1)	2.72	6.50 ± 0.9
AT2G35980	Late embryogenesis abundant hydroxyproline-rich glycoprotein (YLS9)	2.32	5.40 ± 1.0
AT5G26170	Putative WRKY transcription factor 50 (WRKY50)	3.62	7.80 ± 1.5
AT4G27410	NAC domain-containing protein 72 (RD26)	2.33	5.40 ± 1.2
AT4G17490	Ethylene response factor subfamily B-3 of ERF/AP2 transcription factor family (ERF6)	2.54	6.00 ± 1.1
AT2G32020	GCN5-related N-acetyltransferase-like protein	3.53	8.37 ± 1.5
AT3G63060	F-box protein (EDL3)	2.03	6.22 ± 0.8

[a]Fold change is the mean of three independent experiments with the ratio of raw signal values in *igr2-9* and wild-type plants.
[b]Gene expression levels were quantified by real-time PCR and the relative expression rate (RER) was compared between *igr2-9* and wild-type plants. Data represent means ± *SD* ($n = 3$).

that regulate senescence? ROS are proposed to play an essential role in leaf senescence. Indeed, previous studies showed that ROS accumulate during leaf senescence (Navabpour et al. 2003; Khanna-Chopra 2012) and high levels of ROS are present in the chloroplasts of ageing plants (Munné and Alegre 2002). In addition, several *SAGs* are known to be induced in response to oxidative stress (Miller et al. 1999; Navabpour et al. 2003). The connection between oxidative stress and leaf senescence is further supported by the finding that mutants with delayed leaf senescence, such as *ore1*, *ore3/ein2*, *ore9*, and *gigantea*, are resistant to oxidative stress (Kurepa et al. 1998; Woo et al. 2004), while mutants with accelerated leaf senescence, such as *old5*, *aaf-OX*, and *Cdf1*, are associated with disturbed cellular redox balance or hypersensitivity to oxidative stress (Schippers et al. 2008; Chen et al. 2011; Cui et al. 2013). Recent genetic evidence suggests that altered ROS levels likely act as signals that are implemented in the developmental program of the leaf, causing early onset of senescence (Foyer and Noctor 2005; Queval et al. 2007; Zentgraf and Hemleben 2008; Smykowski et al. 2010). In this study, we observed an early leaf senescence phenotype in *GR2* RNAi plants after the leaves were exposed to high levels of H_2O_2 (Figure 7). We also observed an early leaf senescence phenotype in *GR2* RNAi plants after a senescence-inducing dark treatment, which caused H_2O_2 to accumulate (Figure 8). In addition, we showed that considerable levels of H_2O_2 had already accumulated in the young leaves of *GR2* RNAi plants and that H_2O_2 peaked in leaves 30 d after emergence (Figure 6). At this stage, however, an apparent senescence phenotype was not visible and there were no significant

differences in the physiological parameters for leaf senescence between *GR2* RNAi and wild-type plants (Figure 4). More importantly, the results from the microarray analysis show that genes involved in "leaf senescence" and "oxidative stress" were overrepresented in the leaves of *GR2* RNAi plants at 20 d after leaf emergence (Figure 9), suggesting that the senescence- and stress-related genes were already induced at the developmental stage before senescence.

To investigate how GR2 regulates leaf senescence, we compared the transcriptome of the *igr2-9* line with that of wild-type *Arabidopsis* at different developmental stages before the onset of leaf senescence (Breeze et al. 2011) (Figure S4 and Table S3). We analyzed the upregulated genes of transcriptome datasets from the report by Breeze et al. (2011) using GO::TermFinder as described in this study. We showed that the expression of genes related to response to oxidative stress", "response to ROS", "defense response", and "leaf senescence" is significantly overrepresented during the early stages of leaf senescence in wild-type *Arabidopsis*, similar to the finding for *igr2-9*. Breeze et al. (2011) showed that ROS response genes are induced early in leaf senescence. Most of these ROS response genes differ from those induced in *igr2-9*; 51 ROS response genes were upregulated 29 d after sowing (Breeze et al. 2011) and 41 ROS response genes were upregulated in *igr2-9*, but only 13 overlapped. However, these overlapping genes include some important senescence-related genes, such as *NAC2/ORE1/ANAC092* and *SAG21* (Table S3). We investigated if elevated H_2O_2 induced the expression of H_2O_2 marker genes, such as glycosyltransferase family 61 protein, heat shock protein 17.6A, GSTU9, PAD3, WRKY53, and GSTU24, in *igr2-9* plants (Vanderauwera et al. 2005; Gadjev et al. 2006; Queval et al. 2007; Sewelama et al. 2014). Indeed, we observed that these H_2O_2 marker genes were upregulated in the leaves of *igr2-9* plants at 20 d after emergence (Table 2). We also observed the induction of *WRKY53*, *NAC2*, and *SEN1* in *igr2-9* plants before senescence (Table 1). *WRKY53*, *SEN1*, and *NAC2* are marker genes for leaf senescence. It has been shown that WRKY53 and its regulators are induced by ROS (Zentgraf et al. 2010). WRKY53 positively regulates developmental senescence and *wrky53* knock-out mutants exhibit a delayed senescence phenotype. WRKY53 regulates senescence-associated gene expression and acts at an upstream position in the WRKY signaling cascade (Miao et al. 2004). *SEN1* expression is associated with *Arabidopsis* leaf senescence and *SEN1* is induced by oxidative stresses (Oh et al. 1996; Woo et al. 2004). The *NAC2/ORE1/ANAC092* loss-of-function mutant shows a delayed leaf-senescence syndrome, whereas overexpression of *AtNAC2* induces early senescence (Oh et al. 1997; Kim et al. 2009; Balazadeh et al. 2010). Taken together, these results suggest that the elevated accumulation of H_2O_2 in the leaves of *GR2* RNAi plants acts a signal mediator for early leaf senescence.

H_2O_2 can be produced in different cellular compartments, such as chloroplasts, mitochondria, peroxisomes, and the cytoplasm. H_2O_2 pools in different cell compartments may have different effects on leaf senescence. Chloroplasts are thought to be the main target of age-associated oxidative stress in plants (Munńe-Bosch and Alegre 2002) and play a principal role in the regulation of leaf senescence (Zapata et al. 2005; Martínez et al. 2008). Peroxisomes and the ROS generated in these organelles play a central role in natural and dark-induced senescence in pea plants (del Río et al. 1998). Downregulation of *CAT2* in peroxisomes, which results in accumulation of H_2O_2 activates leaf senescence (Zimmermann et al. 2006; Smykowski et al. 2010). H_2O_2 produced in peroxisomes upregulates genes involved in protein repair responses, whereas H_2O_2 produced in chloroplasts induces early signaling responses, by upregulating the expression of transcription factors and biosynthetic genes involved in the production of secondary signaling messengers (Sewelam et al. 2014). Cytoplasmic H_2O_2 also induces leaf senescence, and it appears to have a greater role in senescence signaling than does peroxisomal H_2O_2 (del Río et al. 1998; Bieker et al. 2012). GR2 localizes to both chloroplasts and mitochondria (Creissen et al. 1995; Chew et al. 2003). Since most of the GR activity is in the chloroplast (Edwards et al. 1990; Ding et al. 2009), it is proposed that accumulated H_2O_2 in *GR2* RNAi plants resulted mainly from chloroplasts. *Arabidopsis* plants overexpressing glycolate oxidase in the chloroplast (*GO5*) represent an excellent system in which to study the action of H_2O_2 as a signal molecule in chloroplasts (Fahnenstich et al. 2008). Recently, Sewelam et al. (2014) investigated H_2O_2 signaling from the chloroplast using *GO5* plants. They found that genes related to "oxidative stress", defense response", "leaf senescence", and "phytohormone pathways" were overrepresented in *GO5* plants after 8 h of H_2O_2 production (Figure S5). They also found that H_2O_2 from chloroplasts induces early signaling responses, upregulating the expression of many transcription factors (Sewelam et al. 2014). Indeed, we observed that the expression of many transcription factors was induced in the *igr2-9* line (Table S2). NAC and WRKY transcription factors were shown to be the two largest groups of transcription factors differentially expressed in the senescence transcriptome (Guo et al. 2004). Some of

Table 2. Induction of H_2O_2 marker transcripts in the fourth rosette leaves at 20 d after emergence in the *igr2-9* line

AGI number	Description	Fold change[a]	RER[b]
AT3G10320	Glycosyltransferase family 61 protein	2.20	5.81 ± 1.7
AT5G12030	Heat shock protein 17.6A	1.84	3.22 ± 0.8
AT5G62480	Glutathione S-transferase tau 9 (GSTU9)	4.25	8.43 ± 2.0
AT3G26830	Cytochrome P450 71B15 (PAD3)	2.25	6.70 ± 1.3
AT4G23810	WRKY transcription factor 53 (WRKY53)	2.27	5.97 ± 1.6
AT1G17170	Glutathione S-transferase TAU 24 (GSTU24)	1.66	4.01 ± 1.8

[a]Fold change is the mean of three independent experiments with the ratio of raw signal values in *igr2-9* and wild-type plants.
[b]Gene expression levels were quantified by real-time PCR and the relative expression rate (RER) was compared between *igr2-9* and wild-type plants. Data represent means $\pm$ *SD* ($n = 3$).

these transcription factors have been shown to be central regulators of senescence in wheat and *Arabidopsis* (Miao et al. 2004; Guo and Gan 2006; Uauy et al. 2006; Balazadeh et al. 2010, 2011; Breeze et al. 2011; Yang et al. 2011). Many NAC and WRKY transcription factors were induced in *igr2-9* and *GO5* plants (Table S4). Thus, H_2O_2 pools in the chloroplasts of *GR2* RNAi plants may regulate leaf senescence. GR2 also localizes to mitochondria. The decreased GR2 in *GR2* RNAi plants may cause H_2O_2 to accumulate in mitochondria. Our results show that leaf senescence was accelerated in RNAi plants under dark conditions (Figure 8). Therefore, H_2O_2 in mitochondria and possibly also in peroxisomes may promote dark-induced leaf senescence in *GR2* RNAi plants (del Río et al. 1998).

Recent studies demonstrated that glutathione status is central to the regulation of cell signaling under optimal and stress conditions (Noctor et al. 2012, 2013; Mhamdi et al. 2013; Schnaubelt et al. 2015). Is the early leaf senescence in *GR2* RNAi plants associated with changes in glutathione status? Studies of the *cat2* knockout mutant under photorespiratory conditions showed that glutathione status plays an important role in the H_2O_2-dependent induction of salicylic acid and jasmonic acid signaling pathways (Mhamdi et al. 2010, 2013; Queval et al. 2012; Han et al. 2013a, 2013b). To explore the role of changes in glutathione status in inducing leaf senescence in *GR2* RNAi plants, we compared the transcriptome datasets of *gr1*, *cad2*, *rml1*, and *cat2* plants with those of *igr2-9* plants. We found that the expression of eight genes involved in jasmonic acid signaling was repressed in the *gr1* mutant, whereas that of seven genes involved in jasmonic acid signaling was upregulated under long-day conditions (Mhamdi et al. 2010; Table S5). The expression of 34 and 58 genes involved in jasmonic acid signaling was repressed and up-regulated, respectively, in the *cad2* mutant, which has impaired glutathione synthesis, under long-day conditions (Han et al. 2013a; Table S6). Due to the limited number of genes upregulated in the *gr1* and *cad2* mutants (Tables S5, S6), we were unable to identify genes associated with specific cellular processes by GO::TermFinder analysis. These results demonstrate that glutathione interacts with the jasmonic acid pathway. Studies of the *cat2 gr1* and *cat2 cad2* double mutants showed that glutathione status affects the ability of H_2O_2 to activate the pathogenesis-related jasmonic acid and salicylic acid signaling pathways (Han et al. 2013a, 2013b; Mhamdi et al. 2010, 2013). Transcriptome analyses of the *cat2* mutant, which has a modified glutathione status due to increased levels of H_2O_2, and the *rml1* mutant, which has severely impaired glutathione synthesis, showed that genes involved in the jasmonic acid, salicylic acid, ethylene, and abscisic acid pathways as well as pathogenesis-related genes were highly upregulated in both *cat2* and *rml1* (Mhamdi et al. 2010; Schnaubelt et al. 2015) (Figures S6, S7, Tables S7–9). Our results also showed that genes involved in jasmonic acid, salicylic acid, ethylene, and abscisic acid pathways as well as pathogenesis-related genes were overrepresented in *igr2-9* (Figure 9, Tables S7-9). Thus, our results suggest that the glutathione status of *GR2* RNAi plants may affect leaf senescence by modulating phytohormone pathways and the expression of pathogenesis-related genes (Figure 5).

Glutathione is present in almost all cellular compartments, including chloroplasts, mitochondria, peroxisomes, and the cytosol (Mitter 2002). Oxidative stress may drive characteristic changes in the amounts of glutathione in different sub-cellular compartments. Increased intracellular H_2O_2 availability preferentially drives glutathione accumulation in vacuoles and chloroplasts (Queval et al. 2011). We observed a significant increase in H_2O_2 levels and glutathione accumulation in the leaves of *igr2-9* and *igr2-14* plants than in those of the wild type before a leaf age of 30 d after emergence (Figures 5, 6). Whether such an increase in H_2O_2 levels drives the changes in glutathione accumulation in different cellular compartments in *igr2-9* and *igr2-14* plants is not clear. It has been reported that about 70% of total GR activity is in the chloroplast (Edwards et al. 1990) and that decreased chloroplastic GR activity results in significant accumulation of H_2O_2 in chloroplasts (Ding et al. 2009). In addition, increased H_2O_2 drives a substantial increase in GSSG accumulation in the chloroplast (Queval et al. 2011). Therefore, we expect that there should be a significant increase in GSSG accumulation in the chloroplast of *GR2* RNAi plants when H_2O_2 is increased. GSSG accumulation in chloroplasts could reflect oxidation of GSH already present in the chloroplast in *GR2* RNAi plants with increased levels of endogenous H_2O_2 and have important consequences for redox regulation in this compartment. This redox regulation as a signaling mechanism in the chloroplast plays an important role in regulating leaf senescence as discussed above. GR2 also localizes to mitochondria and thus H_2O_2 should also accumulate in mitochondria in *GR2* RNAi plants. Therefore, it is most likely that there is an accumulation of glutathione in mitochondria in *GR2* RNAi plants. Whether and how glutathione accumulation is affected in other subcellular compartments, such as vacuoles, peroxisomes, nuclei, and the cytosol, in *GR2* RNAi plants remains to be determined.

In this study, we showed that decreased GR2 resulted in early onset of age-dependent and dark- and H_2O_2-induced senescence in *Arabidopsis*. Previous studies showed that lines overexpressing chloroplastic GR had a normal phenotype under normal growth conditions in poplar trees, cotton, and tobacco plants, but displayed enhanced resistance to photoinhibition (including chilling-induced photoinhibition) and oxidative stress (Aono et al. 1993; Broadbent et al. 1995; Foyer et al. 1995; Payton et al. 2001; Kornyeyev et al. 2003). These studies suggest that overexpression of chloroplastic GR may protect plants against various environmental stresses. Thus, we propose that *Arabidopsis* lines overexpressing GR2 display a delayed senescence phenotype under environmental stress conditions, but a normal phenotype under normal growth conditions.

In conclusion, we showed that decreased GR2 led to early onset of age-dependent and dark- and H_2O_2-induced leaf senescence. Our results suggest that the elevated levels of H_2O_2 and modified glutathione status in *GR2* RNAi plants act as signals that mediate early leaf senescence. Thus, GR2 is an important regulator of leaf senescence in *Arabidopsis*.

MATERIALS AND METHODS

Plant materials and growth conditions

All of RNAi lines and mutants used in this study were derived from the wild-type *Arabidopsis thaliana* Columbia (Col-0)

ecotype and cultivated in growth chambers with a photosynthetic photon flux density of 100 μmol m^{-2} s^{-1}, a relative humidity of 75%–80%, a temperature of 22 ± 1°C and a photoperiod of 16/8 h light/dark. The T-DNA insertion *gr2* mutant (SALK_040170) was obtained from the *Arabidopsis* Biological Resource Center (ABRC) and PCR was used to confirm homozygosity of *gr2* with the primers GR2LP and GR2RP (see Table S1). For rapid PCR screening of mutants and RNAi plants, genomic DNA was extracted for analysis as described in our previous study (Zhong et al. 2013). Leaf areas were measured using an LI-3000 A Portable Area Meter (LI-Cor).

Analyses of H_2O_2- and dark-induced senescence

For H_2O_2-induced senescence, the fourth rosette leaves at 20 d after emergence were incubated in 3 mM MES buffer (pH 5.8) in the presence of 10 mM H_2O_2 for 3 d. For dark-induced senescence, the fourth rosette leaves at 20 d after emergence were incubated in 3 mM MES buffer (pH 5.8) and then transferred to complete darkness for periods of up to 6 d.

GR activity assay and quantification of GSH content

Glutathione reductase activity was determined by monitoring the rate of GSH formation at 412 nm, as described in our previous study (Ding et al. 2009). The *in vivo* glutathione level was quantified by reverse-phase HPLC after derivatization with monobromobimane, according to established procedures (Strohm et al. 1995).

Physiological assays for leaf senescence

The fourth rosette leaves of individual plants were used to determine physiological parameters for leaf senescence, including chlorophyll content, F_v/F_m, MDA content, and membrane ion leakage. Chlorophyll content and F_v/F_m were measured according to our previous study (Ding et al. 2012). MDA content was measured according to Hodges et al. (1999). Membrane ion leakage was analyzed by monitoring electrolytes released from leaves using a bench-top conductivity meter (CON500, CLEAN Instruments), according to Chen et al. (2011).

Detection and measurement of ROS in leaves

Total leaf H_2O_2 content was determined by spectrometric assay according to the improved method of Veljovic-Jovanovic et al. (2002). Leaves were ground to a fine powder in liquid nitrogen and the powder was extracted in 1 M $HClO_4$ and 5% insoluble PVP. The homogenate was centrifuged at 12,000 *g* for 10 min at room temperature and the supernatant was neutralized with 5 M K_2CO_3 to pH 5.6 in the presence of 50 μL 0.3 M phosphate buffer (pH 5.6). The homogenate was centrifuged at 12,000 *g* for 1 min at room temperature to remove $KClO_4$. The sample was incubated prior to assay for 10 min with 1 U ascorbate oxidase (Sigma, Watford, UK) to oxidize ascorbate and thereby eliminate the interference of ascorbate. The reaction mixture consisted of 0.1 M phosphate buffer (pH 6.5); 3.3 mM 3-(dimethylamino) benzoic acid; 0.07 mM 3-methyl-2-benzothiazolinone hydrazone; and 50 ng horseradish peroxidase (Sigma, Watford, UK). The reaction was initiated by the addition of an aliquot of the sample. The absorbance change at 590 nm was monitored at 25°C. To eliminate lipid peroxide interference, a parallel aliquot for each sample was incubated for 10 min with 1 U catalase (Sigma, Watford, UK) to catalyze H_2O_2. The lipid peroxide content was then determined using the same procedure as described above and subtracted from each sample. For each assay, the H_2O_2 content in the extract was quantified relative to an internal standard.

For *in situ* detection of H_2O_2, detached leaves were vacuum-infiltrated with 1 mg mL^{-1} 3,3′-diaminobenzidine (DAB) solution (pH 3.8) for 5 min and incubated in the dark at room temperature for 6 h (Thordal-Christensen et al. 1997). For in situ detection of $O_2^{\bullet-}$, detached leaves were vacuum-infiltrated with 1 mg mL^{-1} nitroblue tetrazolium (NBT) solution in 10 mM potassium phosphate buffer (pH 7.8) for 5 min and incubated for 20 min in darkness at room temperature (Kawai-Yamada et al. 2004). Stained leaves were cleared by boiling in acetic acid/glycerol/ethanol (1:1:3, v/v/v) solution before photographs were taken. Imaging of singlet oxygen production was performed as described by Flors et al. (2006). Briefly, detached leaves were immersed in 10 mM SOSG (Invitrogen) and 50 mM phosphate buffer (pH 7.5) for 2 h in darkness and then transferred to light conditions for 4 h. Following excitation of SOSG by UV light, fluorescence images were acquired with a charge-coupled device camera (Olympus) with a Green Fluorescent Protein A (GFPA) interference filter in the objective. Fluorescence intensity was determined using ImageJ software (http://rsb.info.nih.gov/ij/) and the background was subtracted from the readings.

Microscopy of developing seeds

Developing seeds were analyzed by microscopy (Leica DMRBE) according to Meinke (1994). Seeds were removed from the siliques of wild-type and heterozygous *gr2* plants and cleared in Hoyer's solution (3.75 g of gum arabic, 50 g of chloral hydrate, and 2.5 mL of glycerol in 15 mL of water). Cleared seeds were then observed by light microscopy (Leica DMRBE) using differential interference contrast.

Antiserum production

For the production of polyclonal antibodies against GR2, the nucleotide sequence encoding a specific part of GR2 was amplified from cDNA (for primers used, see Table S1). The resulting DNA fragment was fused in frame with the N-terminal His affinity tag of pET28a, and the resulting plasmids were transformed into *Escherichia coli* strain BL21 (DE3). The fusion proteins were purified on a nickel-nitrilotriacetic acid agarose resin matrix and polyclonal antibody was raised in rabbit using the purified antigen. In immunoblot analyses, the dilution ratio for the antibody against GR2 was 1:2000.

Immunoblot analysis

Total leaf proteins were separated using 15% SDS polyacrylamide gels containing 6 M urea. After electrophoresis, the proteins were transferred electrophoretically to polyvinylidene difluoride membranes (Amersham Biosciences, Waukesha, Wisconsin, USA), probed with specific primary antibodies, and visualized using the enhanced chemiluminescence method (Ding et al. 2012).

GR2 promoter construction and GUS staining

GR2$_{pro}$*:GUS* was generated by amplifying the 2-kb sequence upstream of the *GR2* translation start sites and subcloning the

fragment into the pCAMBIA 1381Z binary vector (for primers used, GR2pro1 and GR2pro2, see Table S1). Plant samples were incubated in staining solution (50 mM sodium phosphate buffer, pH 7.2, 0.2% Triton X-100, 10 mM potassium ferrocyanide, 10 mM potassium ferricyanide, and 1 mM 5-bromo-4-chloro-3-indolyl-b-D-glucuronic acid, cyclohexylammonium salt) at 37°C overnight. Samples were then washed in 70% ethanol before photographs were taken (Zhong et al. 2013).

RNAi and complementation of the *gr2* mutant

To obtain RNAi plants, the partial coding region for *GR2* (at3g54660) was amplified with igr2 sense and igr2 antisense primers (Table S1) and cloned into the pKANNIBAL vector between the XbaI-HindIII sites in the sense orientation and the XhoI-EcoRI sites in the antisense orientation. The construct generated in pKANNIBAL was subcloned as a NotI fragment into pART27. The resultant construct was transformed into the *Agrobacterium tumefaciens* GV3101 strain and introduced into *Arabidopsis* plants (Ding et al. 2009). For complementation of *gr2*, the cDNA containing the coding region of *GR2* was amplified by PCR with atgr2 primers (Table S1) and subcloned into the plant expression vector pCAMBIA1301 under the control of P35S. The resulting plasmid was introduced into heterozygous *gr2* plants.

RNA isolation and real-time PCR

Total RNA was isolated using TRIZOL reagent (Sigma–Aldrich) according to the manufacturer's instructions. Next, 500 ng of total RNA was used as template to generate the first-strand cDNA in a 100 μL reaction with the Superscript II cDNA synthesis system (Invitrogen), according to the manufacturer's instructions. The resulting cDNA samples were used for real-time PCR using M×3000P (Stratagene) with SYBR Green I (Invitrogen), according to the manufacturers' protocols. Primer pairs for real-time PCR were designed with the open-source PCR primer design program DNAMAN version 1.1.10 around an intron to obtain a PCR product of 200 to 400 bp. The primer sequences are available in Table S1. The presence of a single PCR product was verified by melt-curve analysis and gel electrophoresis.

Microarray analysis

Microarray analysis was conducted using commercial oligonucleotide microarrays (Genechip *Arabidopsis* ATH1 genome arrays, Affymetrix). Three biological replicates were used for both wild-type and *igr2-9* plants. Each replicate (200 mg) was based on the fourth leaves with an age of 20 d after emergence. Standard Affymetrix protocols were followed throughout. The data were analyzed using GeneSpring GX 11.00. A change in signal of at least twofold compared with the wild type was considered meaningful, if present in all three biological replicates. The distribution of gene ontology (GO) annotations of genes upregulated in *igr2-9* plants was processed using the web-based program at TAIR (http://www.arabidopsis.org). GO-specific terms were investigated using GO::TermFinder (Boyle et al. 2004). *P*-values were calculated using Fisher's test (Agresti 1992). Statistical analysis was carried out using Student's *t*-test. A significant difference between the control and experimental groups was considered with $P<0.01$.

ACKNOWLEDGEMENTS

This study was supported by the National Natural Science Foundation of China (30970218) and the State Key Basic Research and Development Plan of China (2015CB150105). We thank the ABRC for the seed stocks.

REFERENCES

Agresti A (1992) A survey of exact inference for contingency tables. **Stat Sci** 7: 131–153

Alscher RG (1989) Biosynthesis and antioxidant function of glutathione in plants. **Physiol Plant** 77: 457–464

Aono M, Kubo A, Saji H, Tanaka KK, Kondo N (1993) Enhanced tolerance to photooxidative stress of transgenic *Nicotiana tabacum* with chloroplastic glutathione reductase activity. **Plant Cell Physiol** 34: 129–135

Aono M, Saji H, Fujiyama K, Sugita M, Kondo N, Tanaka K (1995) Decrease in activity of glutathione reductase enhanced paraquat sensitivity in transgenic *Nicotiana tabacum*. **Plant Physiol** 107: 645–648

Asada K (1999) The water-water cycle in chloroplasts: Scavenging active oxygen species and dissipation of excess photons. **Annu Rev Plant Physiol Plant Mol Biol** 50: 601–639

Balazadeh S, Hamad S, Allu AD, Matallana-Ramirez LP, Caldana C, Mehrnia M, Zanor MI, Köhler B, Mueller-Roeber B (2010) A gene regulatory network controlled by the NAC transcription factor ANAC092/AtNAC2/ORE1 during salt-promoted senescence. **Plant J** 62: 250–264

Bieker S, Riester L, Stahl M, Franzaring J, Zentgraf U (2012) Senescence-specific alteration of hydrogen peroxide levels in *Arabidopsis thaliana* and oilseed rape spring variety *Brassica napus* L. cv. Mozart. **J Integr Plant Biol** 54: 540–554

Boyle EI, Weng S, Gollub J, Jin H, Botstein D, Cherry JM, Sherlock G (2004) GO::TermFinder-Open source software for accessing Gene Ontology information and finding significantly enriched Gene Ontology terms associated with a list of genes. **Bioinformatics** 20: 3710–3715

Breeze E, Harrison E, McHattie S, Hughes L, Hickman R, Hill C, Kiddle S, Kim YS, Penfold CA, Jenkins D, Zhang C, Morris K, Jenner C, Jackson S, Thomas B, Tabrett A, Legaie R, Moore JD, Wild DL, Ott S, Rand D, Beynon J, Denby K, Mead A, Buchanan-Wollaston V (2011) High-resolution temporal profiling of transcripts during *Arabidopsis* leaf senescence reveals a distinct chronology of processes and regulation. **Plant Cell** 23: 873–894

Broadbent P, Creissen GP, Kular B, Wellburn AR, Mullineaux PM (1995) Oxidative stress responses in transgenic tobacco containing altered levels of glutathione reductase activity. **Plant J** 8: 247–255

Buchanan-Wollaston V, Page T, Harrison E, Breeze E, Lim PO, Nam HG, Lin JF, Wu SH, Swidzinski J, Ishizaki K, Leaver CJ (2005) Comparative transcriptome analysis reveals significant differences in gene expression and signalling pathways between developmental and dark/starvation-induced senescence in *Arabidopsis*. **Plant J** 42: 567–585

Cairns NG, Pasternak M, Wachter A, Cobbett CS, Meyer AJ (2006) Maturation of *Arabidopsis* seeds is dependent on glutathione biosynthesis within the embryo. **Plant Physiol** 141: 446–455

Chen GH, Liu CP, Chen SCG, Wang LC (2011) Role of *ARABIDOPSIS A-FIFTEEN* in regulating leaf senescence involves response to reactive oxygen species and is dependent on *ETHYLENE INSENSITIVE2*. **J Exp Bot** 62: 1–18

Chew O, Whelan J, Millar AH (2003) Molecular definition of the ascorbate-glutathione cycle in *Arabidopsis* mitochondria reveals dual targeting of antioxidant defenses in plants. **J Biol Chem** 278: 46869–46877

Creissen GP, Reynolds H, Xue Y, Mullineaux PM (1995) Simultaneous targeting of pea glutathione reductase and of a bacterial fusion protein to chloroplasts and mitochondria in transgenic tobacco. **Plant J** 8: 167–175

Cui MH, Ok SH, Yoo KS, Jung KW, Yoo SD, Shin JS (2013) An *Arabidopsis* cell growth defect factor-related protein CRS, promotes plant senescence by increasing the production of hydrogen peroxide. **Plant Cell Physiol** 54: 155–167

del Rio LA, Pastori GM, Palma JM, Sandalio LM, Sevilla F, Corpas FJ, Jimenez A, Lopez-Huertas E, Hernandez JA (1998) The activated oxygen role of peroxisomes in senescence. **Plant Physiol** 116: 1195–1200

Ding SH, Lei M, Lu QT, Zhang AH, Yin Y, Wen XG, Zhang LX, Lu CM (2012) Enhanced sensitivity and characterization of photosystem II in transgenic tobacco plants with decreased chloroplast glutathione reductase under chilling stress. **Biochim Biophys Acta** 1817: 1979–1991

Ding SH, Lu QT, Zhang Y, Yang ZP, Wen XG, Zhang LX, Lu CM (2009) Enhanced sensitivity to oxidative stress in transgenic tobacco plants with decreased glutathione reductase activity leads to a decrease in ascorbate pool and ascorbate redox state. **Plant Mol Biol** 69: 577–592

Edwards EA, Rawsthorne S, Mullineaux PM (1990) Subcellular distribution of multiple forms of glutathione reductase in leaves of pea (*Pisum sativum* L.). **Planta** 180: 278–284

Fahnenstich H, Scarpeci TE, Valle EM, Flügge UI, Maurino VG (2008) Generation of hydrogen peroxide in chloroplasts of *Arabidopsis* overexpressing glycolate oxidase as an inducible system to study oxidative stress. **Plant Physiol** 148: 719–729

Flors C, Fryer MJ, Waring J, Reeder B, Bechtold U, Mullineaux PM, Nonell S, Wilson MT, Baker NR (2006) Imaging the production of singlet oxygen in vivo using a new fluorescent sensor, Singlet Oxygen Sensor Green. **J Exp Bot** 57: 1725–1734

Foyer CH, Lelandais M, Galap C, Kunert KJ (1991) Effects of elevated cytosolic glutathione reductase activity on the cellular glutathione pool and photosynthesis in leaves under normal and stress conditions. **Plant Physiol** 97: 863–872

Foyer CH, Noctor G (2005) Redox homeostasis and antioxidant signaling: A metabolic interface between stress perception and physiological responses. **Plant Cell** 17: 1866–1875

Foyer CH, Noctor G (2009) Redox regulation in photosynthetic organisms: Signaling, acclimation, and practical implications. **Antioxid Redox Signal** 11: 861–905

Foyer CH, Souriau N, Perret S, Lelandais M, Kunert KJ, Pruvost C, Jouanin L (1995) Overexpression of the glutathione reductase but not glutathione synthetase leads to increases in antioxidant capacity and resistance to photoinhibition in poplar trees. **Plant Physiol** 109: 1047–1057

Gadjev I, Vanderauwera S, Gechev TS, Laloi C, Minkov IN, Shulaev V, Apel K, Inzé D, Mittler R, Breusegem FV (2006) Transcriptomic footprints disclose specificity of reactive oxygen species signaling in *Arabidopsis*. **Plant Physiol** 141: 436–445

Guo Y, Cai Z, Gan S (2004) Transcriptome of *Arabidopsis* leaf senescence. **Plant Cell Environ** 27: 521–549

Guo Y, Gan S (2006) AtNAP, a NAC family transcription factor, has an important role in leaf senescence. **Plant J** 46: 601–612

Han Y, Chaouch S, Mhamdi A, Queval G, Zechmann B, Noctor G (2013a) Functional analysis of *Arabidopsis* mutants points to novel roles for glutathione in coupling H_2O_2 to activation of salicylic acid accumulation and signaling. **Antioxid Redox Signal** 18: 2106–2121

Han Y, Mhamdi A, Chaouch S, Noctor G (2013b) Regulation of basal and oxidative stress-triggered jasmonic acid-related gene expression by glutathione. **Plant Cell Environ** 36: 1135–1146

Hodges DM, De Long JM, Forney CF, Prange RK (1999) Improving the thiobarbituric acid-reactive-substances assay for estimating lipid peroxidation in plant tissues containing anthocyanin and other interfering compounds. **Planta** 270: 604–611

Jiménez A, Hernandez JA, Pastori G, del Rio LA, Sevilla F (1998) Role of the ascorbate-glutathione cycle of mitochondria and peroxisomes in the senescence of pea leaves. **Plant Physiol** 118: 1327–1335

Kataya ARA, Reumann S (2010) *Arabidopsis* glutathione reductase1 is dually targeted to peroxisomes and the cytosol. **Plant Signal Behav** 5: 171–175

Kawai-Yamada M, Ohori Y, Uchimiya H (2004) Dissection of *Arabidopsis* Bax inhibitor-1 suppressing Bax-, hydrogen peroxide-, and salicylic acid-induced cell death. **Plant Cell** 16: 21–32

Khanna-Chopra R (2012) Leaf senescence and abiotic stresses share reactive oxygen species-mediated chloroplast degradation. **Protoplasma** 249: 469–481

Kim J, Woo R, Kim J, Lim P, Lee I, Choi S, Hwang D, Nam H (2009) Trifurcate feed-forward regulation of age-dependent cell death involving miR164 in *Arabidopsis*. **Science** 323: 1053–1057

Kornyeyev D, Logan BA, Payton P, Allen RD, Holaday AS (2003) Elevated chloroplastic glutathione reducatase activities decrease chilling-induced photoinhibition by increasing rates of photochemistry, but not thermal energy dissipation, in transgenic cotton. **Funct Plant Biol** 30: 101–110

Kurepa J, Smalle J, Va M, Montagu N, Inzé D (1998) Oxidative stress tolerance and longevity in *Arabidopsis*: The late-flowering mutant *gigantea* is tolerant to paraquat. **Plant J** 14: 759–764

Li H, Wang G, Liu S, An Q, Zheng Q, Li B, Li Z (2014) Comparative changes in the antioxidant system in the flag leaf of early and normally senescing near-isogenic lines of wheat (*Triticum aestivum* L.). **Plant Cell Rep** 33: 1109–1120

Lim P, Kim H, Nam H (2007) Leaf senescence. **Annu Rev Plant Biol** 58: 115–136

Lin J, Wu S (2004) Molecular events in senescing *Arabidopsis* leaves. **Plant J** 39: 612–628

Martínez DE, Costa ML, Guiamet JJ (2008) Senescence-associated degradation of chloroplast proteins inside and outside the organelle. **Plant Biol** 10: 15–22

Marty L, Siala W, Schwarzländer M, Fricker MD, Wirtza M, Sweetlove LJ, Meyer Y, Meyer AJ, Reichheld JP, Hell R (2009) The NADPH-dependent thioredoxin system constitutes a functional backup for cytosolic glutathione reductase in *Arabidopsis*. **Proc Natl Acad Sci USA** 106: 9109–9114

Meinke DW (1994) Seed development in *Arabidopsis thaliana*. In: Meyerowitz EM, Somerville CR, eds. *Arabidopsis*. Cold spring Harbor Laboratory Press, New York. pp. 253–259

Mhamdi A, Han Y, Noctor G (2013) Glutathione-dependent phytohormone responses: Teasing apart signaling and antioxidant functions. **Plant Signal Behav** 8: e24181

Mhamdi A, Hager J, Chaouch S, Queval G, Han Y, Taconnat L, Saindrenan P, Gouia H, Issakidis-Bourguet E, Renou JP, Noctor G (2010) *Arabidopsis* GLUTATHIONE REDUCTASE1 plays a crucial role in leaf responses to intracellular hydrogen peroxide and in

ensuring appropriate gene expression through both salicylic acid and jasmonic acid signaling pathways. **Plant Physiol** 153: 1144–1160

Miao Y, Laun T, Zimmermann P, Zentgraf U (2004) Targets of the WRKY53 transcription factor and its role during leaf senescence in *Arabidopsis*. **Plant Mol Biol** 55: 853–867

Miller JD, Arteca RN, Pell EJ (1999) Senescence-associated gene expression during ozone-induced leaf senescence in *Arabidopsis*. **Plant Physiol** 120: 1015–1024

Mittler R (2002) Oxidative stress, antioxidants and stress tolerance. **Trends Plant Sci** 7: 405–410

Munné-Bosch S, Alegre L (2002) Plant ageing increases oxidative stress in chloroplasts. **Planta** 214: 608–615

Navabpour S, Morris K, Allen R, Harrison E, A-H-Mackerness S, Buchanan-Wollaston V (2003) Expression of senescence-enhanced genes in response to oxidative stress. **J Exp Bot** 54: 2285–2292

Noctor G, Foyer CH (1998) Ascorbate and glutathione: Keeping active oxygen under control. **Annu Rev Plant Physiol Plant Mol Biol** 49: 249–279

Noctor G, Gomez L, Vanacker H, Foyer CH (2002) Interactions between biosynthesis, compartmentation and transport in the control of glutathione homeostasis and signalling. **J Exp Bot** 53: 1283–1304

Noctor G, Mhamdi A, Chaouch S, Han Y, Neukermans J, Marquez-Garcia B, Queval G, Foyer CH (2012) Glutathione functions in plants: An integrated overview. **Plant Cell Environ** 35: 454–484

Noctor G, Mhamdi A, Queval G, Foyer CH (2013) Regulating the redox gatekeeper: Vacuolar sequestration puts glutathione disulfide in its place. **Plant Physiol** 163: 665–671

Oh S, Lee S, Chung I, Lee C, Nam H (1996) A senescence-associated gene of *Arabidopsis thaliana* is distinctively regulated during natural and artificially induced leaf senescence. **Plant Mol Biol** 30: 739–754

Oh S, Park J, Lee G, Paek K, Park S, Nam H (1997) Identification of three genetic loci controlling leaf senescence in *Arabidopsis thaliana*. **Plant J** 12: 527–535

Pavet V, Olmos E, Kiddle G, Mowla S, Kumar S, Antoniw J, Alvarez ME, Foyer CH (2005) Ascorbic acid deficiency activates cell death and disease resistance responses in *Arabidopsis*. **Plant Physiol** 139: 1291–1303

Payton P, Webb R, Kornyeyev D, Allen R, Holaday AS (2001) Protecting cotton photosynthesis during moderate chilling at high light intensity by increasing chloroplastic antioxidant enzyme activity. **J Exp Bot** 52: 2345–2354

Queval G, Issakidis-Bourguet E, Hoeberichts FA, Vandorpe M, Gakiére B, Vanacker H, Miginiac-Maslow M, Breusegem FV, Noctor G (2007) Conditional oxidative stress responses in the *Arabidopsis* photorespiratory mutant *cat2* demonstrate that redox state is a key modulator of day length-dependent gene expression, and define photoperiod as a crucial factor in the regulation of H_2O_2-induced cell death. **Plant J** 52: 640–657

Queval G, Jaillard D, Zechmann B, Noctor G (2011) Increased intracellular H_2O_2 availability preferentially drives glutathione accumulation in vacuoles and chloroplasts. **Plant Cell Environ** 34: 21–32

Queval G, Neukermans J, Vanderauwera S, Van Breusegem F, Noctor G (2012) Day length is a key regulator of transcriptomic responses to both CO_2 and H_2O_2 in *Arabidopsis*. **Plant Cell Environ** 35: 374–387

Schippers JHM, Nunes-Nesi A, Apetrei R, Hille J, Fernie AR, Dijkwel PP (2008) The *Arabidopsis* onset of leaf death5 mutation of quinolinate synthase affects nicotinamide adenine dinucleotide biosynthesis and causes early ageing. **Plant Cell** 20: 2909–2925

Schnaubelt D, Queval G, Dong Y, Diaz-Vivancos P, Makgopa ME, Howell G, Simone AD, Bai J, Hannah MA, Foyer CH (2015) Low glutathione regulates gene expression and the redox potentials of the nucleus and cytosol in *Arabidopsis thaliana*. **Plant Cell Environ** 38: 266–279

Sewelama N, Jaspert N, Kelen KVD, Tognetti VB, Schmitz J, Frerigmanne H, Stahl E, Zeier J, Frank Van Breusegem FV, Maurino VG (2014) Spatial H_2O_2 signaling specificity: H_2O_2 from chloroplasts and peroxisomes modulates the plant transcriptome differentially. **Mol Plant** 7: 1191–1210

Smykowski A, Zimmermann P, Zentgraf U (2010) G-box binding factor1 reduces CATALASE2 expression and regulates the onset of leaf senescence in *Arabidopsis thaliana*. **Plant Physiol** 153: 1321–1331

Strohm M, Jouanin L, Kunert KJ, Pruvost C, Polle A, Foyer CH, Rennenberg H (1995) Regulation of glutathione synthesis in leaves of transgenic poplar (*Populus tremula X P. alba*) overexpressing glutathione synthetase. **Plant J** 7: 141–145

Thordal-Christensen H, Zhang Z, Wei Y, Collinge DB (1997) Subcellular localization of H_2O_2 in plants: H_2O_2 accumulation in papillae and hypersensitive response during the barley-powdery mildew interaction. **Plant J** 11: 1187–1194

Tzafrir I, Pena-Muralla R, Dickerman A, Berg M, Rogers R, Hutchens S, Sweeney TC, McElver J, Aux G, Patton D, Meinke D (2004) Identification of genes required for embryo development in *Arabidopsis*. **Plant Physiol** 135: 1206–1220

Uauy C, Distelfeld A, Fahima T, Blechl A, Dubcovsky J (2006) A *NAC* gene regulating senescence improves grain protein, zinc, and iron content in wheat. **Science** 314: 1298–1301

Vanderauwera S, Zimmermann P, Rombauts S, Vandenabeel S, Langebartels C, Gruissem W, Inzé D, Breusegem FV (2005) Genome-wide analysis of hydrogen peroxide-regulated gene expression in *Arabidopsis* reveals a high light-induced transcriptional cluster involved in anthocyanin biosynthesis. **Plant Physiol** 139: 806–821

Veljovic-Jovanovic S, Noctor G, Foyer CH (2002) Are leaf hydrogen peroxide concentrations commonly overestimated? The potential influence of artefactual interference by tissue phenolics and ascorbate. **Plant Physiol Biochem** 40: 501–507

Weaver LM, Gan S, Quirino B, Amasino RM (1998) A comparison of the expression patterns of several senescence-associated genes in response to stress and hormone treatment. **Plant Mol Biol** 37: 445–469

Woo H, Kim J, Nam H, Lim P (2004) The delayed leaf senescence mutants of *Arabidopsis*, *ore1*, *ore3*, and *ore9* are tolerant to oxidative stress. **Plant Cell Physiol** 45: 923–932

Yang SD, Seo PJ, Yoon HK, Park CM (2011) The *Arabidopsis* NAC transcription factor VNI2 integrates abscisic acid signals into leaf senescence via the *COR/RD* genes. **Plant Cell** 23: 2155–2168

Yu X, Pasternak T, Eiblmeier M, Ditengou F, Kochersperger P, Sun JQ, Wang H, Rennenberg H, Teale W, Paponov I, Zhou WK, Li CY, Li XG, Palme K (2013) Plastid-localized glutathione reductase2-regulated glutathione redox status is essential for *Arabidopsis* root apical meristem maintenance. **Plant Cell** 25: 4451–4468

Zapata JM, Guéra A, Esteban-Carrasco A, Martín M, Sabater B (2005) Chloroplasts regulate leaf senescence: Delayed senescence in transgenic *ndhF*-defective tobacco. **Cell Death Differ** 12: 1277–1284

Zentgraf U, Hemleben V (2008) Molecular cell biology: Are reactive oxygen species regulators of leaf senescence? **Prog Bot** 69: 117–138

Zentgraf U, Laun T, Miao Y (2010) The complex regulation of WRKY53 during leaf senescence of *Arabidopsis thaliana*. **Eur J Cell Biol** 89: 133–137

Zimmermann P, Heinlein C, Orendi G, Zentgraf U (2006) Senescence-specific regulation of catalases in *Arabidopsis thaliana* (L.) Heynh. **Plant Cell Environ** 29: 1049–1060

Zhong LL, Zhou W, Wang HJ, Ding SH, Lu QT, Wen XG, Peng LW, Zhang LX, Lu CM (2013) Chloroplast small heat shock protein HSP21 interacts with plastid nucleoid protein pTAC5 and is essential for chloroplast development in *Arabidopsis* under heat stress. **Plant Cell** 25: 2925–2943

SUPPORTING INFORMATION

Additional supporting information may be found in the online version of this article at the publisher's web-site.

Figure S1. Gene structure of At3g54660 and microscopy analysis of developing embryos in the siliques of wild-type and heterozygous *gr2* plants

Figure S2. ROS levels in wild-type (wt) and *GR2* RNAi (*igr2-7*, *igr2-9*, and *igr2-14*) plants during leaf development

Figure S3. Expression of *GR2* is induced by elevated H_2O_2 levels and continuous darkness

Figure S4. Analysis of genes upregulated during the early stages of leaf development in *Arabidopsis* by specific GO terms

Figure S5. Analysis of genes specifically upregulated after 8 h of H_2O_2 production in leaf chloroplasts in *Arabidopsis* over-expressing glycolate oxidase in the chloroplast

Figure S6. Analysis of genes up-regulated in *cat2* following induction of glutathione oxidation after transfer from high CO_2 to ambient air

Figure S7. Analysis of genes upregulated in shoots of the 7-day-old *rootmeristemless1-1 (rml1-1)* mutant

Table S1. List of primers used in this study

Table S2. Genes found to be significantly ($P<0.01$) upregulated (≥ 2, A) or downregulated (≤ 2, B) in *igr2-9* in a microarray analysis

Table S3. Comparative analysis of the genes enriched in specific GO terms between the transcriptomes of leaves of *igr2-9* and wild-type *Arabidopsis* at 29 d after sowing (DAS)

Table S4. List of NAC and WRKY transcription factors induced in the leaves of *igr2-9* and *GO5* (with overexpressed glycolate oxidase in the chloroplast) plants

Table S5. Genes induced in the leaves of *gr1* plants grown under long-day conditions

Table S6. Genes induced in the leaves of *cad2* plants grown under long-day conditions

Table S7. Comparative analysis of the upregulated genes enriched in specific GO terms between the transcriptomes of leaves of *igr2-9* and *cat2* plants grown under short-day (SD) conditions

Table S8. Comparative analysis of the upregulated genes enriched in specific GO terms between the transcriptomes of leaves of *igr2-9* and *cat2* plants grown under long-day (LD) conditions

Table S9. Comparative analysis of the upregulated genes enriched in specific GO terms between the transcriptomes of leaves of *igr2-9* and *rml1* plants